AD NUMBER

ADB008137

NEW LIMITATION CHANGE

TO

Approved for public release, distribution unlimited

FROM

Distribution authorized to U.S. Gov't. agencies only; Test and Evaluation; 28 NOV 1975. Other requests shall be referred to Electronic Systems Division, Hanscom AFB, MA 01731.

AUTHORITY

ESD USAF ltr, 17 Dec 1981

AD-B008137

Technical Note

1975-59

Application of Adaptive Filtering Methods to Maneuvering Trajectory Estimation

C. B. Chang
R. H. Whiting
M. Athans

24 November 1975

Prepared for the Ballistic Missile Defense Program Office, Department of the Army, under Electronic Systems Division Contract F19628-76-C-0002 by

Lincoln Laboratory

MASSACHUSETTS INSTITUTE OF TECHNOLOGY

LEXINGTON, MASSACHUSETTS

The work reported in this document was performed at Lincoln Laboratory, a center for research operated by Massachusetts Institute of Technology. This program is sponsored by the Ballistic Missile Defense Program Office, Department of the Army; it is supported by the Ballistic Missile Defense Advanced Technology Center under Air Force Contract F19628-76-C-0002.

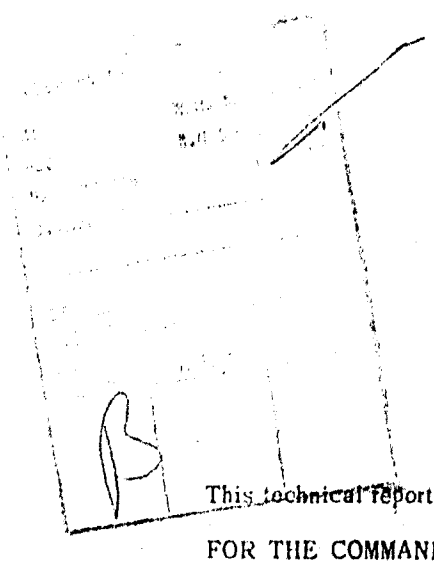

This technical report has been reviewed and is approved for publication.

FOR THE COMMANDER

Eugene C. Raabe

Eugene C. Raabe, Lt. Col., USAF
Chief, ESD Lincoln Laboratory Project Office

MASSACHUSETTS INSTITUTE OF TECHNOLOGY

LINCOLN LABORATORY

APPLICATION OF ADAPTIVE FILTERING METHODS TO MANEUVERING TRAJECTORY ESTIMATION

C. B. CHANG
R. H. WHITING
M. ATHANS

Group 32

TECHNICAL NOTE 1975-59

24 NOVEMBER 1975

LEXINGTON MASSACHUSETTS

ABSTRACT

The purpose of this report is to examine several modifications of extended Kalman filters which can be used to estimate the position, velocity, and other key parameters asscciated with maneuvering re-entry vehicles. These filters will be described and discussed in terms of the fundamental problems of modeling accuracy, filter sophistication, and the real-time computational requirements. A nine-state, extended Kalman filter based upon the maneuvering vehicle dynamics is compared with several other candidate filters. These candidate filters include a simple filter based upon polynomial dynamics decoupled with respect to the coordinates and a more complex, fully coupled, seven-state, extended Kalman filter based upon a ballistic re-entry vehicle dynamics. Techniques which adaptively increase the process noise to compensate for modeling errors during the manevuers are examined.

TABLE OF CONTENTS

ACKNOWLEDGMENT

The authors would like to thank Dr. John Tabaczynski for reviewing the manuscript with helpful suggestions, Leonard Youens for programming support, and Tina Marshall for typing.

1. INTRODUCTION

Estimating the state and associated parameters (i.e., tracking) of a re-entry vehicle (RV) based on its radar measurements is a highly complex problem in nonlinear estimation. Not only does the vehicular nonlinear equation of motion represent an excessive computational burden, but the necessity of identifying key parameters associated with vehicle dynamics complicates the problem even further. The application of the linear Kalman filter[1] and its extension to the nonlinear case[2,3] for the tracking of a ballistic re-entry vehicle (BRV) has been studied extensively during the past decade.[4-11] Although many filters have been discussed, they can generally be divided into two categories, i.e., filters based upon polynomial modeled dynamics (referred to as polynomial filters) and filters based upon the vehicular nonlinear differential equation of motion (referred to as BRV filters). There exists a trade-off between these two types of filters in both performance and computational requirements.[6]

In many practical applications of recursive estimation theory, there is a problem in obtaining an exact representation of the dynamic process. In the BRV tracking context, the BRV filter suffers from the fact that the ballistic coefficient which must be identified on-line is an unknown and time-varying parameter. For a moderate parameter variation, the ballistic coefficient is often modeled as a constant state variable with the variations and

uncertainties compensated for by a ficticious process noise term.[2,4] The variance of this noise term is related to the system structure and the variation of the parameter and can be determined on-line by adaptive filtering methods or premission by extensive simulation studies. This technique has been applied successfully in estimating the ballistic coefficient of a ballistic re-entry vehicle.[7-10]

The problem of state and parameter estimation of a maneuvering re-entry vehicle (MARV) has received scant attention in the past. A subject which has been discussed in some detail pertains to the tracking of maneuvering aircraft[12,13] and linear state dynamics is usually assumed. The MARV tracking problem is similar to the maneuvering aircraft tracking problem in the sense that the target maneuvering force represents uncertain dynamics in the equation of motion. In this paper, several versions of the extended Kalman filter which can be used to estimate the position, velocity, and other key parameters associated with a MARV are discussed. Similar to the BRV tracking case, the basic problem is still one of trading off the factors of improved modeling accuracy, filter sophistication, and computational requirements.

Three filters are discussed. The most complex one is the extended Kalman filter based upon a MARV differential equation of motion (referred to as the MARV filter). There are nine states in this filter, i.e., position (3-state), velocity (3-state), drag (1-state), and lift (2-state). In this case the fictitious

noise components affect only the drag and lift parameters. The second filter is a modified BRV filter. It utilizes the BRV equation of motion but adaptively changes the process noise level to compensate for the modeling error. The last filter is a polynomial filter also with adaptive process noise. The method of adaptive filtering utilized in these last two filters is based upon that of Jazwinski.[14] The performance of these filters is compared in terms of bias and RMS errors developed through Monte Carlo exercise of the algorithm. Trajectories with different levels of maneuvering severity are used to examine sensitivity of performance with respect to the size of maneuver. In addition since a MARV initially re-enters along a ballistic trajectory, a BRV filter may be used initially with a subsequent switch to a MARV filter upon detection of a vehicle maneuver. This approach referred to as a combined filter is not examined in detail, nowever, a generalized likelihood ratio test for maneuver identification is described.

The MARV differential equation of motion is defined in a rectangular (Cartesian) coordinated system. A dish radar is assumed located at the center of the coordinate system. The measurement variables of the dish radar include range, azimuth, and elevation. The rectangular coordinate system has the property that it makes the trajectory differential equations less complicated. The disadvantage is that the measurement equations are

nonlinear in terms of the state variables. The rectangular coordinate is employed here because it is better suited for understanding the geometry of the vehicle maneuver.

This report is organized as follows. The MARV differential equations of motion are presented in the next section. The generalized maximum-likelihood ratio test for maneuver detection is presented in the third section. The extended Kalman filter equations specific to the MARV tracking problem are presented in Section 4. Section 5 presents a review of adaptive filtering methods. Special emphasis is given to Jazwinski's adaptive filtering method with application to the tracking problem. A brief review of other adaptive filtering methods and a discussion on the feasibility of their applications to the tracking problem are included. Section 6 presents numerical performance results of the described filters for simulated test data. Comparisons of both bias and RMS estimation errors for position, velocity, and parameters are presented. The last section presents a discussion of our investigation thus far and the direction for future development.

2. MODELING OF MARV DYNAMICS

In this section, the MARV differential equation of motion is presented. A Cartesian coordinate system is employed to describe these equations because it is felt that this system is better suited for "physical" understanding. A flat, nonrotating

earth with constant gravity model is assumed. For the altitude region below 100 km which is our concern, this assumption introduces only insignificant modeling errors while greatly simplifying the equations. When the vehicle is viewed as a point mass re-entering along a ballistic trajectory, there are two significant force terms, gravity and aerodynamic drag, acting on the vehicle. The drag force acts opposite to the velocity vector with a magnitude proportional to the air density and the square of the velocity. When the vehicle undertakes a maneuver, a third force term , lift, is introduced. The lift force is in a plane perpendicular to the velocity vector. It may be represented by the magnitude and the direction angle.

The MARV equations are stated below.*

$$\dot{V}_x = -\tfrac{1}{2}\rho\alpha(1+\lambda^2)V_xV-\tfrac{1}{2}\rho\delta\lambda\frac{V_xV_zV^2}{V_p^2}\sin\gamma$$

$$-\mathrm{SGN}(\gamma)\tfrac{1}{2}\rho\delta\lambda\frac{V_yV^2}{V_p^2}\sqrt{V^2\cos^2\gamma-V_z^2}$$

$$\dot{V}_y = -\tfrac{1}{2}\rho\alpha(1+\lambda^2)V_yV-\tfrac{1}{2}\rho\delta\lambda\frac{V_yV_zV^2}{V_p^2}\sin\gamma$$

$$+\mathrm{SGN}(\gamma)\tfrac{1}{2}\rho\delta\lambda\frac{V_xV^2}{V_p^2}\sqrt{V^2\cos^2\gamma-V_z^2}$$

$$\dot{V}_z = -\tfrac{1}{2}\rho\alpha(1+\lambda^2)V_zV+\tfrac{1}{2}\rho\lambda V^2\sin\gamma-G \qquad (2.1)$$

*For derivation, see the Appendix.

where

V_x, V_y, V_z: velocity components along x,y,x axis, respectively

V: magnitude of velocity

$$\left(= \sqrt{v_x^2 + v_y^2 + v_z^2}\right)$$

V_p: planar velocity $\left(= \sqrt{v_x^2 + v_y^2}\right)$

α: drag force proportionality constant, its inverse is known as the ballistic coefficient which is the ratio of vehicle mass to effective drag area

δ: lift force proportionality constant, it has a similar aerodynamic meaning as drag

λ: a constant defining the lift induced drag

γ: angle between lift vector and the local horizontal plane. It has the following convention

γ positive → climb
γ negative → dive

$-90° < \gamma < 90°$ → left turn
$90° < \gamma < 270°$ → right turn

$SGN(\gamma)$: $SGN(\gamma) = 1$ for $-90° < \gamma < 90°$
-1 otherwise

ρ: air density

G: gravitational constant

Notice that when all the lift-related parameters are zero (i.e., λ, δ, γ), the above set of equations reduce to the ballistic trajectory equations. Similar to the ballistic vehicle case, the extended Kalman filter based upon the above model would include position,

velocity, and unknown parameters as state variables. This state augmentation method for parameter identification has been applied successfully when the parameter undergoes moderate variation.[2] Ideally, one would like to identify all the MARV parameters, namely δ, γ, and λ. However, this makes the augmented system unobservable.* A reduced-order model will be used to identify a combination of these parameters. This involves estimating the tangential deceleration constant $\alpha(1+\lambda^2)$, the normal deceleration constant $\lambda\delta$, and the angle γ. This makes the MARV estimator a nine-state filter with position (3-state), velocity (3-state), and three lift/drag parameters [$\alpha(1+\lambda^2)$, $\lambda\delta$, and γ] as state variables.

The lift force representation used in these equations is defined strictly in keeping with the aerodynamics. A disadvantage of this model is that the angle parameter γ is related to the vehicle acceleration in a "very" nonlinear fashion (i.e., sine, cosine, square root, etc.). A method to make the parameter relationship appear more "linear" is to decompose the lift force on an appropriate coordinate system and then estimate the magnitude along the coordinates. This formulation enables the lift parameters to relate to the acceleration terms in a manner similar to that of the drag parameter in the BRV case. One such possible

*The observability theory for a general nonlinear system has not been found. For the particular system studied here, it can be shown that it is indeed impossible to separate all parameters unless other relations can be specified.

decomposition which maintains the lift force perpendicular to the drag force defines a lift force parallel to the ground (the turn force) and another force perpendicular to the turn force (the climb force). With this formulation, the MARV equations may be rewritten as:

$$\dot{V}_x = -\tfrac{1}{2}\rho V V_x \alpha(1+\lambda^2) - \tfrac{1}{2}\rho V^2 \lambda\delta_t \frac{V_y}{V_p} - \tfrac{1}{2}\rho V \lambda\delta_c \frac{V_x V_z}{V_p}$$

$$\dot{V}_y = -\tfrac{1}{2}\rho V V_y \alpha(1+\lambda^2) + \tfrac{1}{2}\rho V^2 \lambda\delta_t \frac{V_x}{V_p} - \tfrac{1}{2}\rho V \lambda\delta_c \frac{V_y V_z}{V_p}$$

$$\dot{V}_z = -\tfrac{1}{2}\rho V V_z \alpha(1+\lambda^2) + \tfrac{1}{2}\rho V V_p \lambda\delta_c - G \qquad (2.2)$$

where δ_c and δ_t are climbing and turning parameters, respectively, with the following sign convention

$\delta_c > 0 \rightarrow$ climbing, $\quad \delta_c < 0 \rightarrow$ diving

$\delta_t > 0 \rightarrow$ left $\quad \delta_t < 0 \rightarrow$ right turn

Notice that the total lift force constant is represented by $\lambda\delta = \lambda\sqrt{\delta_t^2+\delta_c^2}$.

The nine-state MARV filter presented in the later section is the extended Kalman filter based upon Eq. (2.2). The actual parameters estimated are $\alpha_d = \alpha(1+\lambda^2)$, $\alpha_t = \lambda\delta_t$, and $\alpha_c = \lambda\delta_c$.

3. MANEUVER DETECTION

In this section, a likelihood ratio test for maneuver detection is presented. Maneuvering vehicles initially re-enter

along a ballistic trajectory. If a maneuver is initiated while the target is being tracked by a ballistic filter, biases will begin to build up in the filter residual.* The maneuver detection is designed to exploit this residual bias. A bias model which is increased linearly with time is assumed. If the amount of bias is known a priori to the detector, the detection problem is simplified to distinguish two Gaussian processes with known means and variances. This simple case is first introduced to establish notation. When the bias is unknown, and this is usually the case in practice, a generalized likelihood ratio test is formulated.[15] This is shown to be an extension of the known bias case. When the bias function is assumed completely unknown, the test is reduced to the well-known chi-square test. This case is shown in the last subsection.

3.1 Known Bias Case

Assume the bias in the residual caused by a vehicle maneuver during one measurement interval be known to the hypothesis tester and let it be denoted by $\underline{\Delta y}$. It is assumed using our assumption of a linearly increasing bias, the bias after k measurements is $k\underline{\Delta y}$. Let a stack of K measurements be collected for testing and $\underline{\Delta \tilde{y}}_k$ denote the k-th measurement residual with covariance $P_{r,k}$. Two hypothesis representing MARV (H_1) and BRV (H_o) are

*"Filter residual" is defined as the difference of the measurement and the predicted measurement.

$$H_1: \quad \underset{\sim}{\Delta\tilde{y}}_k = k\underset{\sim}{\Delta y} + \underset{\sim}{n}_k \qquad , \quad k=1,\ldots,K \tag{3.1}$$

$$H_o: \quad \underset{\sim}{\Delta\tilde{y}}_k = \underset{\sim}{n}_k$$

where the noise term $\underset{\sim}{n}_k$ is assumed Gaussian with zero mean and covariance $P_{r,k}$ and is uncorrelated for different k. The likelihood test is given by

$$\Lambda = \frac{p(\underset{\sim}{\Delta\tilde{y}}_1,\ldots,\underset{\sim}{\Delta\tilde{y}}_k/H_1)}{p(\underset{\sim}{\Delta\tilde{y}}_1,\ldots,\underset{\sim}{\Delta\tilde{y}}_k/H_o)} \underset{\text{BRV}}{\overset{\text{MARV}}{\gtrless}} \lambda$$

$$= c\cdot\exp\left\{-\frac{1}{2}\sum_{k=1}^{K}\left[(\underset{\sim}{\Delta\tilde{y}}_k - k\underset{\sim}{\Delta y})^T P_{r,k}^{-1} \quad (\underset{\sim}{\Delta\tilde{y}}_k - k\underset{\sim}{\Delta y})\right.\right.$$

$$\left.\left. - (\underset{\sim}{\Delta\tilde{y}}_k)^T P_{r,k}^{-1} (\underset{\sim}{\Delta\tilde{y}}_k)\right]\right\} \underset{\text{BRV}}{\overset{\text{MARV}}{\gtrless}} \lambda \tag{3.2}$$

This equation may be reduced to obtain the following sufficient statistics

$$\ell = \sum_{k=1}^{K} k\underset{\sim}{\Delta y}^T P_{r,k}^{-1} \underset{\sim}{\Delta\tilde{y}}_k - \frac{1}{2}\sum_{k=1}^{K} k^2 \underset{\sim}{\Delta y}^T P_{r,k}^{-1} \underset{\sim}{\Delta y} \tag{3.3}$$

Notice that ℓ is a Gaussian random process with known means and variances under both hypothesis. The performance of this test is well known and is characterized by the normalized separation of these two hypotheses.[11] This separation can be represented by the following definition of "signal-to-noise" ratio:

$$SNR_K = \frac{|E(\ell/H_1) - E(\ell/H_o)|^2}{Var(\ell/H_1) + Var(\ell/H_o)} \tag{3.4}$$

where E( ) denotes the statistical exception and Var( ) the variance of the enclosed event. Subscript "K" denotes the integrated SNR over K measurements. Substituting in the appropriate terms yields

$$SNR_K = \frac{1}{2} \sum_{k=1}^{K} k^2 \underline{\Delta y}^T P_{r,k}^{-1} \underline{\Delta y}$$

$$= SNR_1 \frac{K(K+1)(2K+1)}{6} \tag{3.5}$$

Notice that SNR_K increases rapidly with K.

3.2 Unknown Bias Case

In the more realistic case where the bias term Δy is unknown to the detector, the test becomes a generalized likelihood ratio test which replaces the Δy by its maximum likelihood estimate .[11] This results in the following modified likelihood ratio.

$$\Lambda = \frac{\underset{\Delta y}{\text{Max}}\ p(\underset{\sim}{\Delta y}_1, \ldots, \underset{\sim}{\Delta y}_K / \underline{\Delta y}, H_1)}{p(\underset{\sim}{\Delta y}_1, \ldots, \underset{\sim}{\Delta y}_K / H_o)} \underset{\text{BRV}}{\overset{\text{MARV}}{\gtrless}} \lambda \tag{3.6}$$

Letting $\underline{\Delta \hat{y}}$ denote the maximum likelihood estimate of $\underline{\Delta y}$, Eq. (3.3) becomes

$$\ell = \sum_{k=1}^{K} k \underline{\Delta \hat{y}}^T P_{r,k}^{-1} \underline{\Delta \tilde{y}}_k - \frac{1}{2} \sum_{k=1}^{K} k^2 \underline{\Delta \hat{y}}^T P_{r,k}^{-1} \underline{\Delta \hat{y}} \tag{3.7}$$

The resulting estimate $\underline{\Delta \hat{y}}$ is then given by

$$\underline{\Delta \hat{y}} = \left[\sum_{n=1}^{K} n^2 P_{r,n}^{-1} \right]^{-1} \left[\sum_{n=1}^{K} n P_{r,n}^{-1} \underset{\sim}{\Delta y}_n \right] \tag{3.8}$$

For the case when K=1, Eq. (3.7) becomes

$$\ell = \underset{\sim}{\Delta y}^{T} P_{r,k}^{-1} \underset{\sim}{\Delta y}$$

which is the chi-square statistic.

3.3 Unknown Bias Function Case

In the previous subsections, the bias is assumed to increase linearly in the residual. Higher order relations may also be used in modeling the bias. However, when a small number of measurements are used in the detector, the linear model is a reasonable one to use. One could also assume no knowledge at all about the bias model. In this case the hypothesis test can be stated as

$$\begin{aligned} H_1: \quad & \underset{\sim}{\Delta \tilde{y}_k} = \underset{\sim}{\Delta y_k} + \underset{\sim}{n_k} \\ H_o: \quad & \underset{\sim}{\Delta \tilde{y}_k} = \underset{\sim}{n_k} \end{aligned} \quad , \quad k=1,\ldots,K \tag{3.9}$$

where the change of $\underset{\sim}{\Delta y_k}$ with k is totally unassumed. The generalized likelihood ratio test is

$$\Lambda = \frac{\underset{\underset{\sim}{\Delta y_1},..,\underset{\sim}{\Delta y_K}}{\text{Max}} \; p(\underset{\sim}{\Delta \tilde{y}_1},..,\underset{\sim}{\Delta \tilde{y}_K}/\underset{\sim}{\Delta y_1},..,\underset{\sim}{\Delta y_K},H_1)}{p(\underset{\sim}{\Delta \tilde{y}_1},..,\underset{\sim}{\Delta \tilde{y}_K}/H_o)} \underset{\text{BRV}}{\overset{\text{MARV}}{\gtrless}} \lambda \tag{3.10}$$

The maximum likelihood estimate of $\underset{\sim}{\Delta y_k}$ is therefore $\underset{\sim}{\Delta \hat{y}_k}$ and results in the following sufficient statistic.

$$\ell = \frac{1}{2} \sum_{k=1}^{K} \underset{\sim}{\Delta \tilde{y}_k} P_{r,k}^{-1} \underset{\sim}{\Delta \tilde{y}_k}$$

This is a summation of K chi-square random variables. Detectors may be devised by either testing the above summation or by using a sequential testing process utilizing consecutive chi-square statistics.

4. RADAR TRACKING FILTERS

The function of the tracking filter is to provide estimates of the states and parameters which describe the motion of the re-entry vehicle. These estimates are computed by means of a weighted combination of the predicted and measured target states. The prediction procedure carried out in the filter is based upon the assumed target dynamics and the past tracking data.

Let the following vector differential equation denote the vehicle dynamic model used in the filtering equation

$$\dot{\underline{x}}(t) = \underline{f}(\underline{x}(t)) + \underline{n}(t) \tag{4.1}$$

where $\underline{n}(t)$ is a zero-mean white Gaussian noise process with covariance $Q(t)$. This state driving noise, which is sometimes artificially introduced by the filtering algorithm, is used to compensate for the uncertainties that might exist in the model. The measurements are collected from radar at discrete times and represented by

$$\underline{z}_k = \underline{h}(\underline{x}_k) + \underline{v}_k \tag{4.2}$$

where $\underline{v}_k$ is a zero mean Gaussian noise process with covariance R_k. The observation function $\underline{h}(\cdot)$ represents the transformation from the state space to the measurement space or radar measurement variables. This estimation problem is known as the continuous process-discrete measurement problem.[2]

Numerous algorithms have been proposed for re-entry vehicle tracking.[4-11] They differ mainly in the filter sophistication and the modeling complexity. The most widely used filter structure is still the extended Kalman filter regardless of the target dynamic model assumed. The extended Kalman filter is most popular because it offers an excellent balance between the computational requirements and the overall tracking performance. For this reason, this same basic filter is used for MARV tracking. The extended Kalman filter is stated below in its familiar form:

Predict Cycle

$$\text{(state)} \quad \dot{\hat{\underline{x}}}_{t/k} = \underline{f}(\hat{\underline{x}}_{t/k}) \tag{4.3}$$

$$\text{(covariance)} \quad \dot{P}_{t/k} = F_k P_{t/k} + P_{t/k} F_k^T + Q(t) \tag{4.4}$$

where $\hat{\underline{x}}_{t/k}$ denotes the estimate of $\underline{x}$ at time t based upon all the data up to time t_k and $P_{t/k}$ denotes the covariance of $\hat{\underline{x}}_{t/k}$ at time t conditioned upon all the data up to time t_k. F_k is the Jacobian matrix of $\underline{f}(\underline{x}(t))$ at $\hat{\underline{x}}_{k/k}$. Assuming that the process noise is constant from t_k to t_{k+1}, Eq. (4.4) may be approximated by its discrete equivalent

$$P_{k+1/k} = \Phi_k [P_{k/k} + Q_k \Delta t_k] \Phi_k^T \tag{4.4a}$$

where Φ_k is the transition matrix of F_k and $\Delta t_k = t_{k+1} - t_k$.

Update Cycle

$$\text{(state)} \quad \hat{\underline{x}}_{k+1/k+1} = \hat{\underline{x}}_{k+1/k} + W_{k+1}(\underline{z}_{k+1} - h(\hat{\underline{x}}_{k+1/k})) \tag{4.5}$$

$$\text{(gain)} \quad W_{k+1} = P_{k+1/k} H_{k+1}^T (H_{k+1} P_{k+1/k} H_{k+1}^T + R_{k+1})^{-1}$$

(covariance)

$$P_{k+1/k+1} = (I - W_{k+1} H_{k+1}) P_{k+1/k} \tag{4.6}$$

where H_{k+1} = Jacobian matrix of $\underline{h}(\underline{x}(t))$ at $\hat{\underline{x}}_{k+1/k}$.

The filter residual $\underline{\Delta\tilde{y}}_k$ used in Section 3 is related to the above filtering equation by

$$\underline{\Delta\tilde{y}}_{k+1} = \underline{z}_{k+1} - \underline{h}(\hat{\underline{x}}_{k+1/k})$$

with covariance

$$P_{r,k+1} = H_{k+1} P_{k+1/k} H_{k+1}^T + R_{k+1}$$

When the proper filter optimality conditions are satisfied, the residual $\underline{\Delta\tilde{y}}_{k+1}$ has the same properties as those of the measurement noise process and is known as the innovation process.

Three filters based upon varying degrees of model complexity are discussed in the remaining part of this section. The first two filters are obtained by using a simple modification of existing ballistic vehicle tracking filters. This is made possible by introducing substantial process noise through the filter so that the estimates rely heavier on the measurement than on the target dynamic model. Without this modification, these two filters would diverge quickly from the MARV trajectory. The method of computing the noise variance is based upon that of Jazwinski[14] and is discussed in the next section. The third filter is the extended

Kalman filter based upon the MARV differential equation of motion. All three filters are now discussed individually in their order of complexity.

4.1 Constant Acceleration Model (Polynomial Filter)

The simplest of the three candidate filters is referred to as the "polynomial" filter because the motion for each of the three coordinates is described in a second-order, constant acceleration dynamic model. The parameters to be estimated make up a 9-dimensional state vector,

$$\underline{x}(t) = (x,y,z,\dot{x},\dot{y},\dot{z},\ddot{x},\ddot{y},\ddot{z})^T \tag{4.7}$$

The coordinates are assumed to be decoupled resulting in the simple linear time-invariant state equation,

$$\dot{\underline{x}}(t) = \begin{bmatrix} \underline{0} & \underline{I} & \underline{0} \\ \underline{0} & \underline{0} & \underline{I} \\ \underline{0} & \underline{0} & \underline{0} \end{bmatrix} \underline{x}(t)+\underline{n}(t), \tag{4.8}$$

where $\underline{n}(t)$ represents the process noise term with covariance level to be determined.

Since this filter does not explicitly estimate the drag deceleration, A_D, the nonlinear relationship between the inverse ballistic coefficient, α, and the estimated states, $A_V - g\cos\theta = \frac{1}{2}\rho v^2 \alpha$ is used to generate an estimate of the drag and drag parameters. In this expression A_V is the total acceleration along the velocity

vector, g is the gravitational constant, θ is the angle between the velocity vector and the line-of-sight through the center of the earth, and $\frac{1}{2}\rho v^2$ is the free air-stream pressure. From the experience of using this filter in the ballistic re-entry vehicle tracking, the α estimated is expected to contain a large random error.

4.2 Constant Drag Model (BRV Filter)

The equations-of-motion for a ballistic re-entry vehicle can be obtained from Eq.(2.1) by letting $\delta=0$, $\lambda=0$, and $\gamma=0$. These equations are completely delineated by the 7-dimensional state vector,

$$\underline{x}(t) = (x,y,z,\dot{x},\dot{y},\dot{z},\alpha)^T \tag{4.9}$$

which forms the basic parameter set for the BRV filter.

The inverse ballistic coefficient, α, is the only parameter for which there is no simple, practical model structure in terms of the other parameters. It is modeled as a constant Gaussian Markov process, $\dot{\alpha} = n_\alpha(t)$, where $n_\alpha(t)$ is a zero-mean white noise process. This modeling method is often used in parameter identification.[2]

The filter based upon this dynamic model has been used extensively for real-time BRV tracking in the field with excellent results reported.[7-10] The modification which accommodates this filter to the MARV requires the introduction of a proper process noise term. Due to its fine performance in ballistic vehicle

tracking, it is retained here with the hope that it will still provide satisfactory ballistic coefficient estimates. In addition, it indeed requires only minimum modification to the existing algorithms.

4.3 Constant Drag and Lift Model (MARV Filter)

The most complex and general filter considered in this paper is structured similarly to the BRV filter but with the addition of the lift acceleration parameters to the state vector,

$$\underline{x}(t) = (x,y,z,\dot{x},\dot{y},\dot{z},\alpha_d,\alpha_t,\alpha_c)^T \tag{4.10}$$

and the implementation of the complete MARV equations-of-motion, Eq. (2.2). As in the BRV case, the parameters are modeled as $\dot{\alpha}_d = n_{\alpha_d}$, $\dot{\alpha}_t = n_{\alpha_t}$, $\dot{\alpha}_c = n_{\alpha_c}$ where the noise processes are assumed to be white Gaussian.

This filter may also be used to track a BRV trajectory. In using it to track BRV's, one should expect that the maneuver parameter estimates are only caused by noise. The advantage of using the MARV filter to track the BRV trajectory is that when the RV executes unexpected maneuvering, the filter can adjust automatically and still maintain target track. The disadvantage is that the MARV filter will have poorer estimation performance during the ballistic portion of the re-entry than would the BRV filter. In addition, the redundant states carried along by the MARV filter unnecessarily increase the computational load. One approach to alleviate this problem is to use the BRV filter

initially and switch to the MARV filter after detecting the maneuver. This combined filter is also tested in the simulation study.

5. METHODS OF ADAPTIVE FILTERING

In this section, the characteristics of the appropriate process noise needed to complete the description of the adaptive extended Kalman filter are discussed. Functionally, this noise should reflect those uncertainties or discrepancies between the assumed dynamic model and the actual re-entry phenomena. Pragmatically, the problem is one of selecting noise levels (variances) which are large enough to prevent filter divergence yet small enough to retain the learning potential of the filter model; thus avoiding unnecessarily large RMS errors in the estimates due to a heavier reliance on the individual measurements. As the process noise is increased, the prediction accuracy decreases, thus requiring large radar track gates. In addition, our ability to distinguish between possible interfering targets is diminished.

From the discussion in the previous section, the state augmentation method for parameter estimation (i.e., α_d, α_t, α_c) requires the use of process noise. However, the use of BRV and polynomial filters for MARV tracking requires even higher process noise levels be applied to most states of the target dynamics. The experience gained in determining the process noise for parameter identification in BRV tracking problem and its extension to the MARV tracking is discussed in the first subsection. The

subject of adaptive filtering has been a topic of much research.[14,16-20] A brief discussion of adaptive methods and their applicability to MARV tracking is given in Section 5.2. The application of the adaptive filtering method proposed in Ref. 14 to complement the BRV and polynomial filters for MARV tracking is discussed in Section 5.3.

5.1 Constant Process Noise

The initial criterion for selecting the process noise is to simply ensure track maintenance during worst case conditions, i.e., large measurement variances, substantial nonlinear drag decelerations, and severe evasive maneuvers. The noise covariance matrix is selected prior to the mission and includes only those elements of the matrix corresponding to parameters where we might expect the greatest source of errors. For the polynomial, BRV, and MARV filters, zero-mean Gaussian process noise is added to acceleration rates, $n(t) = (0,0,0,0,0,0,n_{\ddot{x}},n_{\ddot{y}},n_{\ddot{z}})$; drag rates (or equivalently α), $n(t) = (0,0,0,0,0,0,n_{\dot{\alpha}})$; and drag-lift rates, $n(t) = (0,0,0,0,0,0,n_{\alpha_d},n_{\alpha_t},n_{\alpha_c})$, respectively. The variances of these Gaussian processes are selected on a trial-and-error basis by adjusting the levels during simulation exercises until track can be maintained throughout re-entry.

For the BRV filter a procedure which increases the noise level in accordance with the magnitude of the estimated drag deceleration has proven to work quite well for tracking ballistic

re-entry vehicles. This method is motivated by the fact that the major source of error orginates from the drag model and that these model errors become increasingly pronounced as the air density increases in drag; thus, allowing the filter to adapt to the comparatively rapidly changing drag at lower altitudes. For this reason, the process noise for α is defined as $\sigma_\alpha^2 = (c\hat{\alpha})^2$ where a satisfactory value for c (based on experience) is c = 0.1.[7-10]

To date, little is known about the process noise level needed for the other two parameters, α_t and α_c, in the MARV filter. In the simulation study, they are selected to be representative of a uniform distribution of the range of possible parameter variation.

The above process noise selection procedure is of course not "optimal." It represents, however, the result of some limited numerical experience and is easily implemented.

5.2 Optimal Adaptive Filtering

The optimum Kalman filter requires complete knowledge of system dynamics and statistics. A mismatched Kalman filter could ultimately lead to filter divergence.[2] The method which attempts to identify the uncertain part of the system dynamics and statistics on-line with the filtering process is called adaptive filtering. An even more versatile approach is to lump all the modeling uncertainties in the system process noise. This method is certainly nonoptimal in its own right, however, it enables a filter based upon

a poor dynamic model to still lock on to the system output and is the approach used in this paper. Much work has been done in this area in attempting to rigorously and optimally identify the unknown part of the system. In the problem addressed here, we are interested only in identifying the proper process noise variance, $Q(t)$.

Representative work along this line may be found in Refs. 16-20. These methods include use of, 1) the properties of the innovation process,[16-18] 2) the Bayesian formulation which includes the covariance $Q(t)$ in the a posteriori density function,[19] and 3) the correlation-type estimator based upon residuals.[20] All of these methods require extensive computational resources since all the data are iteratively reprocessed for each new estimate. To circumvent some of the computational requirements most of these "optimal" methods are subplanted by some sort of suboptimal algorithm employing simpler estimators and limited memory filters. For most cases these suboptimal algorithms still require unacceptable computer resources yet are of questionable reliability.

Due to processing time constraints we have considered only the simple (even nonoptimum) methods, in this tracking study.

5.3 A Simple Adaptive Filtering Method

Detection of an unexpected maneuver as well as any compensation that may be taken is generally based upon the behavior of the residuals, $\underline{\Delta\tilde{y}}_k$. The covariance matrix of this residual is

computed in the filtering algorithm as

$$P_{r,k} = H_k P_{k/k-1} H_k^T + R_k \tag{5.1}$$

Jazwinski[14] suggested a real-time algorithm which determines the appropriate process noise based upon the statistical behavior of the residuals. The attractiveness of this method is in the simplicity of its implementation. Even though there is no criterion of optimality involved, it is shown in the numerical results that this method enables the BRV and polynomial filter to track the MARV. The original discussion in Ref. 14 pertained to linear filtering, it will be restated here using our notations in nonlinear filtering.

Let $\Sigma_{k/k-1}$ denote the covariance matrix which appears in the prediction cycle due to the process noise, i.e.,

$$\Sigma_{k/k-1} = \Phi_{k-1}(Q_{k-1}\Delta t_{k-1})\Phi_{k-1}^T \tag{5.2}$$

Assuming that the matrix which appears in the residual covariance due to $\Sigma_{k/k-1}$ is diagonal, the Jazwinski estimator states

$$\left[H_k \Sigma_{k/k-1} H_k^T\right]_{ii} = \begin{cases} \frac{1}{\Delta t_k}\left[\underline{\Delta\hat{y}}_k \underline{\Delta\hat{y}}_k^T - P_{r,k}\right]_{ii}; & \text{if positive} \\ 0 \quad ; \quad \text{otherwise} \end{cases} \tag{5.3}$$

This estimator basically requires that the residual must be within a reasonable range of the residual covariance as predicted by the Kalman filter. If it fails to satisfy this requirement, the process noise is increased accordingly to enlarge the corresponding

residual covariance so that the filter update equation places heavier reliance on the most recent measurement.

Ultimately, the Q_k matrix must be determined. In the tracking problem discussed here, one may assume that the position estimation error is caused by the errors from the velocity estimates. For the case of BRV filter, the Q_k matrix becomes

$$Q_k = \left[\begin{array}{c|cccc} \underline{0}^{3x3} & \multicolumn{4}{c}{\underline{0}^{3x4}} \\ \hline & \sigma_{\dot{x}}^2 & 0 & 0 & 0 \\ \underline{0}^{4x3} & 0 & \sigma_{\dot{y}}^2 & 0 & 0 \\ & 0 & 0 & \sigma_{\dot{z}}^2 & 0 \\ & 0 & 0 & 0 & \sigma_{\alpha}^2 \end{array}\right] \tag{5.4}$$

The σ_α^2 of above is determined by the method discussed in Section 5.1 while $\sigma_{\dot{x}}^2$, $\sigma_{\dot{y}}^2$, $\sigma_{\dot{z}}^2$ will be computed from Eqs. (5.2) and (5.3). It is known that the transition matrix Φ may be approximated by the following expression

$$\Phi = \left[\begin{array}{c|cccc} & \Delta t & 0 & 0 & 0 \\ \underline{I}^{3x3} & 0 & \Delta t & 0 & 0 \\ & 0 & 0 & \Delta t & 0 \\ \hline & 1 & 0 & 0 & \phi_1 \\ \underline{0}^{4x3} & 0 & 1 & 0 & \phi_2 \\ & 0 & 0 & 1 & \phi_3 \\ & 0 & 0 & 0 & 1 \end{array}\right] \tag{5.5}$$

where Δt is the time interval between measurements. Using (5.5) and (5.4) and carrying out the multiplication of (5.2) yield

$$\Sigma_{k/k-1} = \begin{bmatrix} \Delta t^2\sigma_{\dot{x}}^2 & 0 & 0 & \Delta t\sigma_{\dot{x}}^2 & 0 & 0 & 0 \\ 0 & \Delta t^2\sigma_{\dot{y}}^2 & 0 & 0 & \Delta t\sigma_{\dot{y}}^2 & 0 & 0 \\ 0 & 0 & \Delta t^2\sigma_{\dot{z}}^2 & 0 & 0 & \Delta t\sigma_{\dot{z}}^2 & 0 \\ \Delta t\sigma_{\dot{x}}^2 & 0 & 0 & \sigma_{\dot{x}}^2+\phi_1^2\sigma_\alpha^2 & \phi_1\phi_2\sigma_\alpha^2 & \phi_1\phi_3\sigma_\alpha^2 & \phi_1\sigma_\alpha^2 \\ 0 & \Delta t\sigma_{\dot{y}}^2 & 0 & \phi_1\phi_2\sigma_\alpha^2 & \sigma_{\dot{y}}^2+\phi_2\sigma_\alpha^2 & \phi_2\phi_3\sigma_\alpha^2 & \phi_2\sigma_\alpha^2 \\ 0 & 0 & \Delta t\sigma_{\dot{z}}^2 & \phi_1\phi_3\sigma_\alpha^2 & \phi_2\phi_3\sigma_\alpha^2 & \sigma_{\dot{z}}^2+\phi_3^2\sigma_\alpha^2 & \phi_3\sigma_\alpha^2 \\ 0 & 0 & 0 & \phi_1\sigma_\alpha^2 & \phi_2\sigma_\alpha^2 & \phi_3\sigma_\alpha^2 & \sigma_\alpha^2 \end{bmatrix} \tag{5.6}$$

The H matrix in (5.3) is the Jacobian matrix of the measurement equations. In the tracking application, it represents the linearized transformation from state variables to the radar measurement variables. With (5.3), one is always able to compute the position component variances in the state space from residuals in the measurement space. Let the position component variance be denoted by σ_x^2, σ_y^2, and σ_z^2, one obtains $\sigma_{\dot{x}}^2 = \sigma_x^2/\Delta t^2$, $\sigma_{\dot{y}}^2 = \sigma_y^2/\Delta t^2$, and $\sigma_{\dot{z}}^2 = \sigma_z^2/\Delta t^2$ from (5.6). This completes the computation of the Q matrix.

Several problems emerge from this rather simple adaptive noise estimator. This estimator as outlined above is based upon a single residual which, as Jazwinski points out, may not be statistically significant. Random fluctuations of the residual could

cause unnecessary response from the estimator. One possible course of action is to use the smoothed residuals over a large number of measurements.

Other approaches of preventing an over-reaction are to do one or some of the following:

1. Activate the adaptive estimator only during a detected maneuver or within an altitude interval over which maneuvering is expected to occur.

2. Limit the amount of noise that may be added--corresponding to the maximum maneuver expected.

3. Change Eq. (5.3) to the form

$$\underline{\Delta\tilde{y}}_k \underline{\Delta\tilde{y}}_k^T - c\, P_{r,k}$$

where "c" is a constant to be determined empirically.

6. NUMERICAL EXAMPLES

In this section the numerical results obtained by applying simulated data to the filters are presented. The simulation program includes a trajectory simulator and the tracking filters. The trajectory simulator consists of a numerical integration program which generates noise-free trajectories in Cartesian coordinates and a radar simulator which transforms the state variables into the radar measurement state space and adds noise to the measurements. There are four algorithms used in the testing. They are the polynomial filter, BRV filter, MARV filter, and the combined BRV and MARV filter. The combined filter uses a nonadaptive

BRV filter initially and switches to a MARV filter after detecting the maneuver. The detection algorithm is that described in Section 3.2. The simulator runs in a Monte Carlo fashion to obtain the means and standard deviations of the estimates. The results from each filter are compared in terms of position rms error, velocity rms error, and the means and standard deviations of parameter estimates. Evaluation of these filters based on real data will not be discussed in this report. Due to the model discrepancies which always arise between a mathematical model and the actual physical process, the validity of applying such techniques to the real world can only be established after a thorough exercise with actual field data. This subject is currently under investigation and will be documented in a future Lincoln Laboratory report.

Three trajectories having different maneuvering scenarios are used to exercise these filters. The first trajectory (T1) can be described as a moderate maneuver in which a combined dive and left turn both having equal magnitude begins at 30 km altitude. The maneuvering force increases gradually to about 128 g at around 23 km and then decreases to zero at about 16 km. At 16 km, the RV initiates a climb and eventually reaches 120 g at around 10 km and decreases to zero at around 5 km. The second trajectory (T2) undergoes more severe maneuvers. It instantaneously jumps to a 160 g left turn at 35 km. The turning coefficient (α_t) is maintained constant until 27 km while the lift force builds to a

maximum of 500 g due primarily to the increase in air density. The left turn force then drops instantly to about 45 g at 27 km and then increases to 152 g at 18 km. At this altitude it reduces to about 20 g and remains small until 3 km. The lift force is zero below this altitude. The ballistic coefficient of T2 also jumps to simulate a sudden change in the lift induced drag force. The T2 trajectory is indeed unrealistic and it is included solely for the purpose of testing filter response. The third trajectory (T3) takes only minor maneuvers. A combined dive and left turn with equal magnitudes starts at 30 km and gradually increases to 5 g at 25 km then decreases to zero at 20 km. At 20 km, the RV initiates a combined climb and right turn with equal magnitudes and eventually reaches 10 g at 15 km and decreases to zero at 10 km. It dives and turns to the left again at 10 km and reaches 10 g at 5 km and decreases to zero at 1 km. This trajectory closely resembles a BRV trajectory. It is included to test the sensitivity of the MARV filter.

A dish radar is assumed located at the origin of the trajectory coordinate system. The measurement variables of a dish radar include range (R), azimuth (A), and evaluation (E). Assuming that the trajectory coordinate system uses x-axis pointing east, and y-axis pointing north, and z-axis perpendicular to the local horizontal plane, the radar measurement variables are related to the state variables by the following equations.

$$R = \sqrt{x^2 + y^2 + z^2}$$

$$A = \tan^{-1} \frac{x}{y} \qquad (6.1)$$

$$E = \tan^{-1} \frac{z}{\sqrt{x^2+y^2}}$$

A range measurement standard deviation of one meter is assumed. For waking targets, a one-meter standard deviation is still representative since coherent burst waveforms can be used for range marking and clutter suppression. The angle measurement standard deviation is assumed to be .17 milliradian. A data rate of 10 measurements per second is utilized throughout the trajectory.

The process noise is introduced in the MARV filter only in the states representing parameters (i.e., α_d, α_t, and α_c). The variance of input noise for α_d is $(.1\hat{\alpha}_d)^2$ just as in the BRV case. The variances of process noise for the other two parameters are determined by the range of parameter variation, the inherent filter stability and the balance of bias and random errors. After testing over a range of values, they were selected to be $5\text{x}10^{-7}$ for T1, $5\text{x}10^{-6}$ for T2, and $5\text{x}10^{-8}$ for T3. The track is initiated at 80 km altitude. The adaptive portion of the BRV and polynomial filters is activated at 45 km.

The estimated position rms errors made by all four algorithms in using trajectories T1, T2, and T3 are presented in Figs.

1, 5, and 9, respectively. All algorithms performed satisfactorily. If the only tracking requirement is to maintain the vehicle in track, the polynomial filter is certainly most attractive since it requires the least computation.

Recalling the fact that the adaptive filtering algorithm enables the filter to rely heavier on current measurements, note the sudden increase of position error at 45 km altitude which indicates the activation of the adaptive feature. If the adaptive filtering algorithm was not used, the BRV filter would diverge quickly from the trajectory. This indicates a trade-off between a range of tolerable rms errors and a range of intolerable bias error (loss of track). Notice that large, impulse-like errors appear with MARV filter and the combined filter in tracking T2 trajectory. As described earlier, the maneuvering force history of T1 is moderate (and realistic). The MARV filter responded to this maneuvering smoothly. The change of maneuvering force of the T2 is sudden and drastic. The impulse-like error of the MARV filter represents the system delay in responding to such a change. The large transients in the combined filter observed on both trajectories occur as one switches from the BRV to the MARV filter. This effect may also be seen in other state estimates as well. The advantage of using this combined algorithm is the better performance achieved and the less computation required during the nonmaneuvering region. Unfortunately, the transient phenomenon

lasts over a 10 km altitude interval. This is due in some respect to the fact that the method used in initiating the MARV filter in the combined algorithm is rather arbitrary. An improved initiation algorithm could smooth the transient somewhat.

The velocity rms errors of using trajectories T1, T2, and T3 are presented in Figs. 2, 6, and 10, respectively. The polynomial filter estimates have the largest errors. The transients in the combined filter are again apparent. The averaged ballistic coefficient estimates of trajectories T1, T2, and T3 are presented in Figs. 3, 7, and 11, respectively. Also shown in these figures are the true underlying parameters and the one standard deviation level. The estimates made by the polynomial filter are very erratic. The estimates made by the MARV filter are very good and follow the parameter variation closely. The combined filter also estimated the coefficient well except during the transition period. The estimates made by the BRV filter exhibit substantial biases in the maneuvering region. It, however, is much more stable than the polynomial estimate. From the one standard deviation interval, it is found that the random errors are usually within 10% of the estimated values except those of the polynomial filter.

Figures 4, 8, and 12 present the maneuvering parameter estimates of trajectories T1, T2, and T3, respectively. Only the MARV filter and the combined filter can provide these estimates. The estimates follow the parameter closely. Notice in Fig. 8 the

turning coefficient takes an abrupt jump while the estimates respond to this change with only about six radar pulse delay. The random error of maneuvering parameter estimates of the T3 trajectory is rather large. Notice that the magnitudes of the maneuvering parameters of this trajectory are small, the estimtes are mostly buried in noise. One could improve the situation by further reducing the process noise level on these parameters. It, however, implies using the a priori knowledge which are usually not available in a real-time tracking application. Figure 13 presents the maneuvering parameter estimates of T3 made by the MARV filter with process noise variances equal to 5×10^{-10}. Notice that the random error is considerably smaller in this case. A useful analysis will be to relate the range of parameter variation, the process noise level, and the estimation rms errors. This analysis may be applied for off-line study of vehicles exercising small maneuvers. The anomalous transient effects of the combined filter can again be seen in these results.

7. CONCLUSIONS

Three basic filters which can be used for the tracking of a maneuvering re-entry vehicle have been presented. They are the extended adaptive Kalman filters based upon MARV, BRV, and polynomial dynamic models. A fourth algorithm which combines the use of a nonadaptive BRV filter and the MARV filter through the application of a generalized maximum likelihood ratio test is also

presented. All algorithms are tested based upon the simulated trajectory data.

From the simulation study, it is found that all filters can track the target successfully in that they all have comparable position estimation errors. If the only tracking objective is to maintain the target in track, the polynomial filter is the most attractive one to use since it requires least computation. The attractiveness of the MARV filter is its ability to provide maneuvering parameter estimates and more accurate ballistic coefficient estimates during target maneuvering. It is shown that the estimates have only small errors and the filter can rapidly follow the severe variations of the underlying true parameters. The disadvantage of using the MARV filter lies in the computational burden imposed on a real-time system. The BRV filter fits somewhere in between in that it does not require as much computation as the MARV filter while still provides a reasonable ballistic coefficient estimate when the target is undergoing maneuvers. It is found that severe transients exist in the combined filter which occur when switching from the BRV to the MARV filter and an appropriate algorithm for handover must be determined.

Much more work still has to be done in exercising these filters on real data. The real data contains properties which may not be fully modeled by mathematics. Such properties include the range measurement degradation due to wake contamination,

uncertainties in angle measurement error modeling, among others. Due to the complexity expanded in the MARV filter, it may be more sensitive to these real data uncertainties mentioned above.

Some fundamental conclusions may also be drawn at this point. It is shown that the extended Kalman filter can perform successfully in estimating the states of a severely nonlinear system. In addition, the state augmentation method for parameter estimation is effective even in systems having large parameter variations. The simple adaptive filtering method employing process noise to compensate for the model uncertainties is extremely powerful. When only the estimates of lower order states (such as position) are desired, large modeling errors may be tolerated with little sacrifice in the performance. These observations are supported with examples shown in this paper. One cannot, of course, claim that these methods work for all nonlinear systems with large parameter variations. They do represent useful methods applicable to many nonlinear systems.[21]

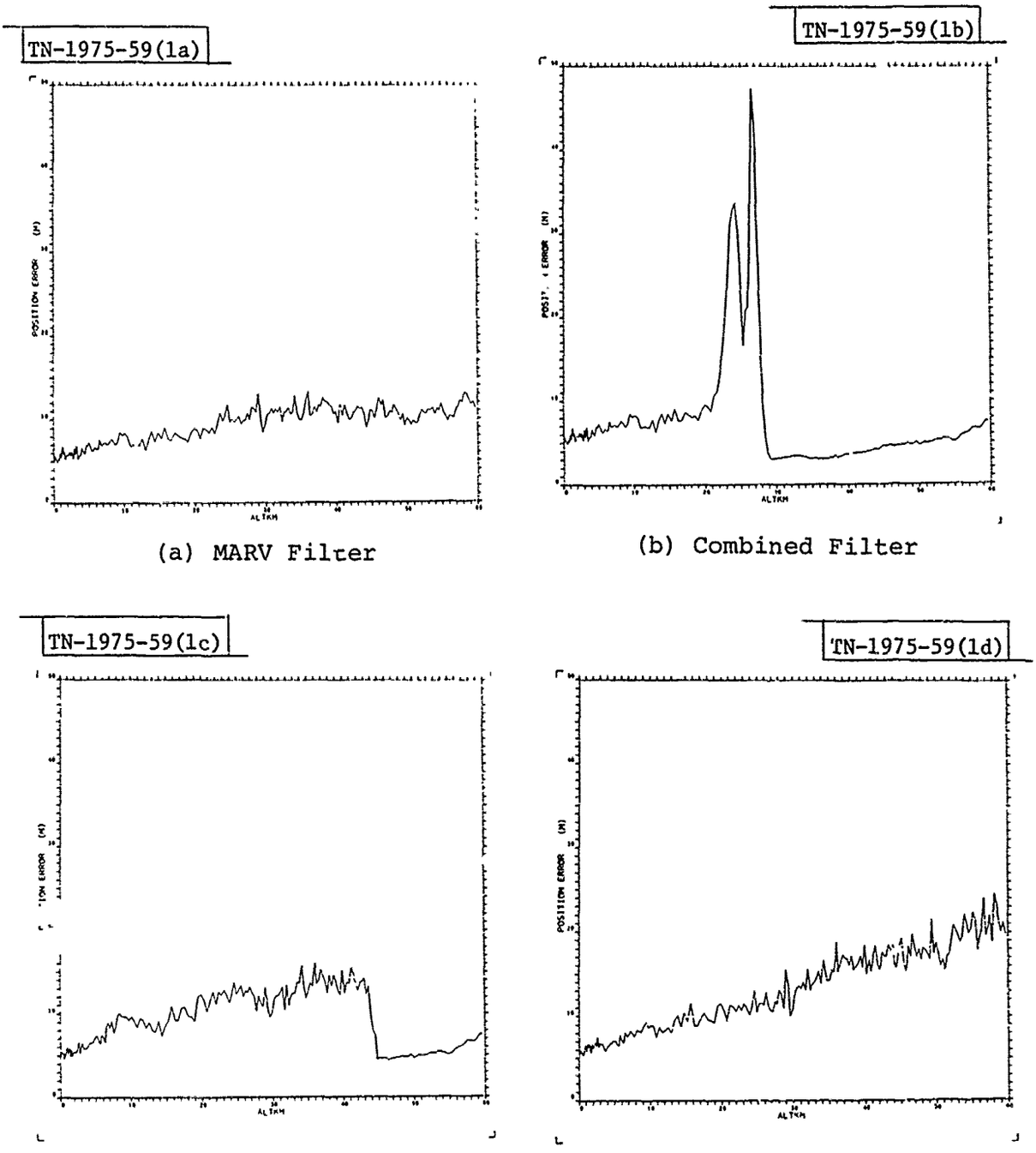

(a) MARV Filter

(b) Combined Filter

(c) BRV Filter

(d) Poly. Filter

Fig. 1. Position estimate rms errors of T1.

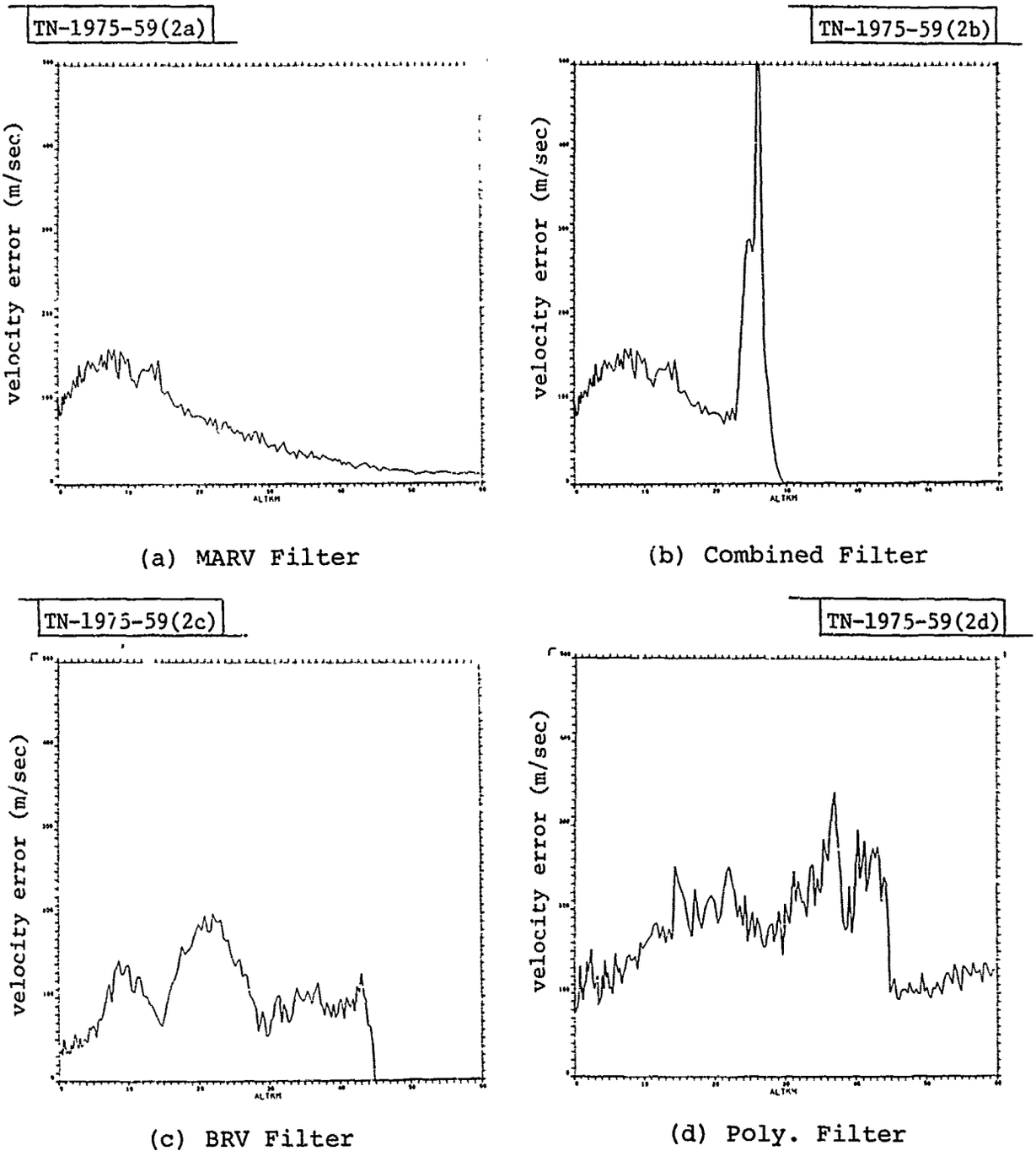

Fig. 2. Velocity estimate rms errors of T1.

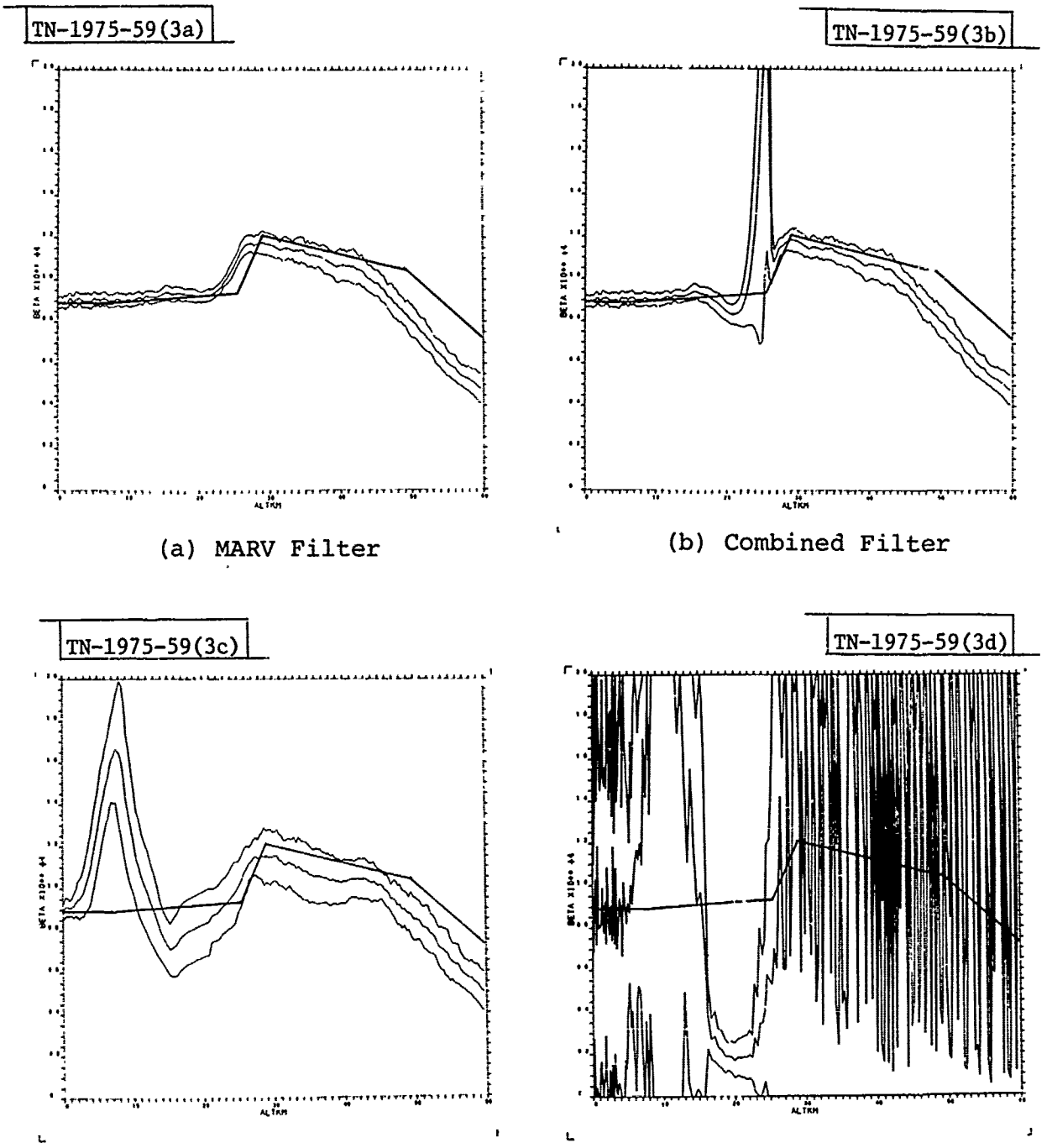

Fig. 3. Ballistic coefficient estimate of T1.

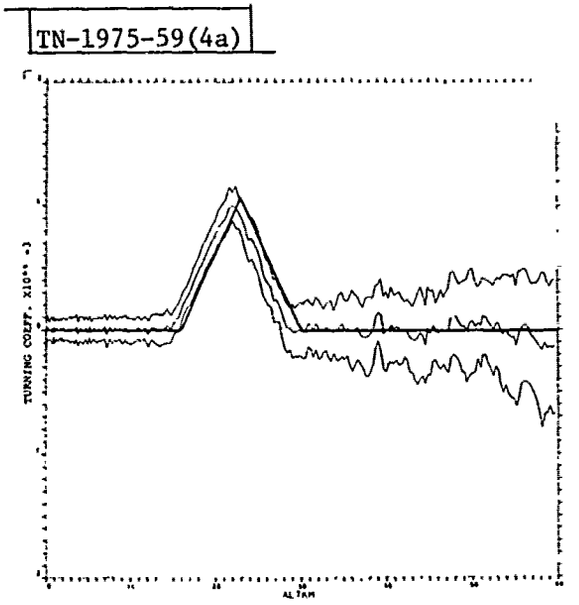

(a) Turning Coefficient Estimate of MARV Filter

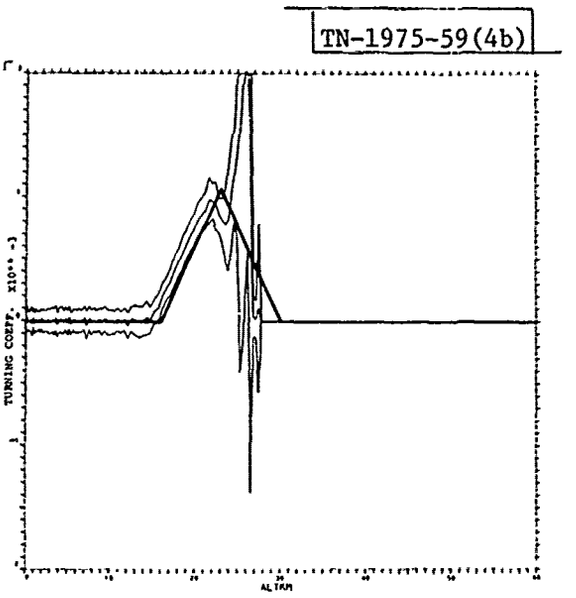

(b) Turning Coefficient Estimate of Combined Filter

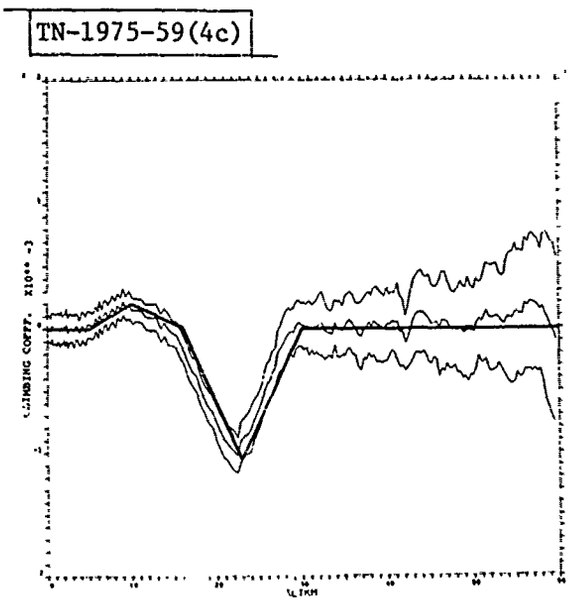

(c) Climbing Coefficient Estimate of MARV Filter

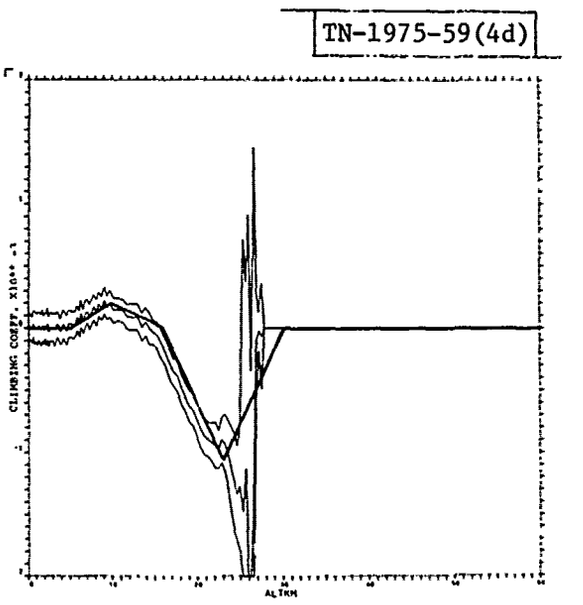

(d) Climbing Coefficient Estimate of Combined Filter

Fig. 4. Maneuvering parameter estimate of T1.

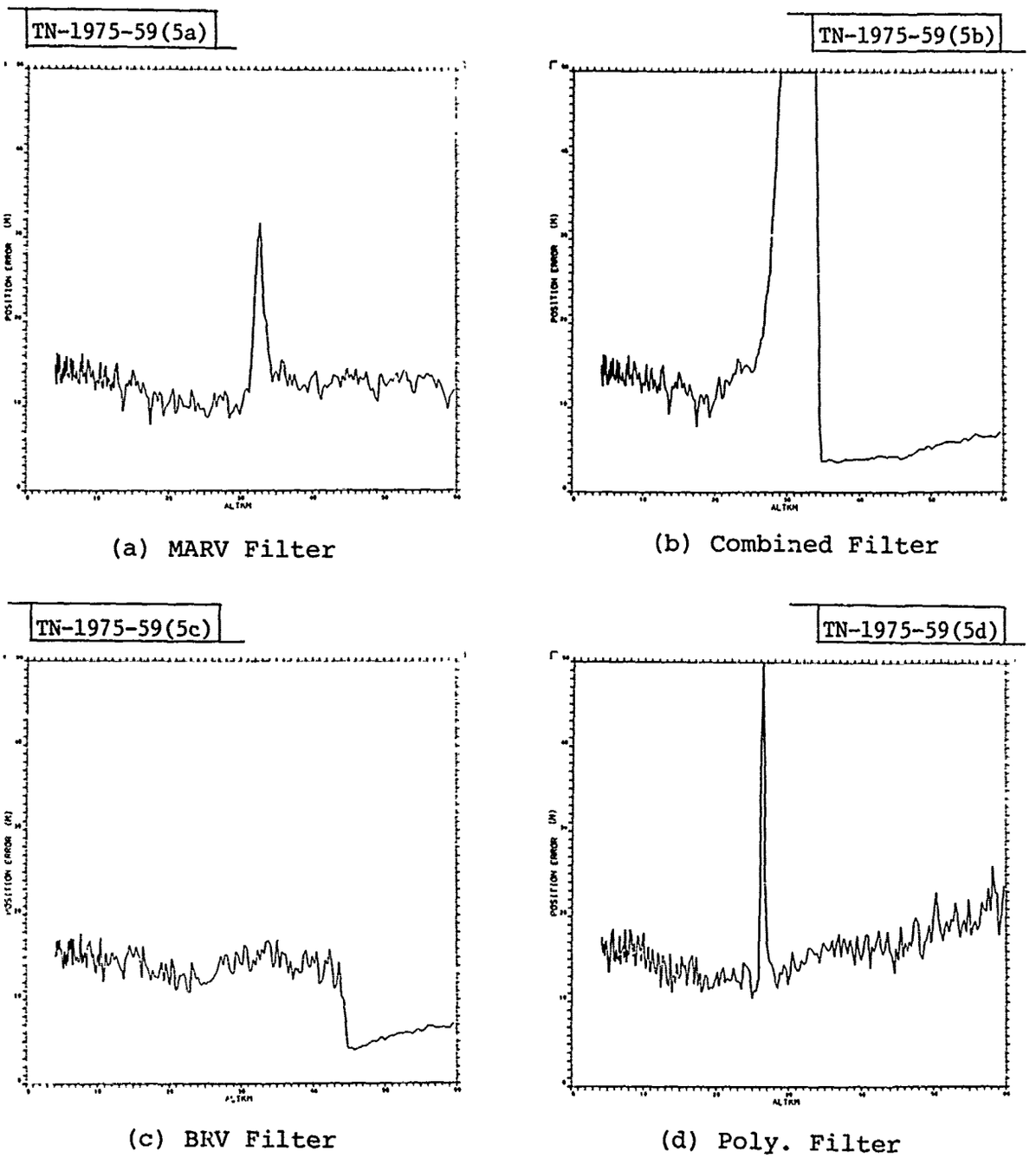

(a) MARV Filter

(b) Combined Filter

(c) BRV Filter

(d) Poly. Filter

Fig. 5. Position estimate rms errors of T2.

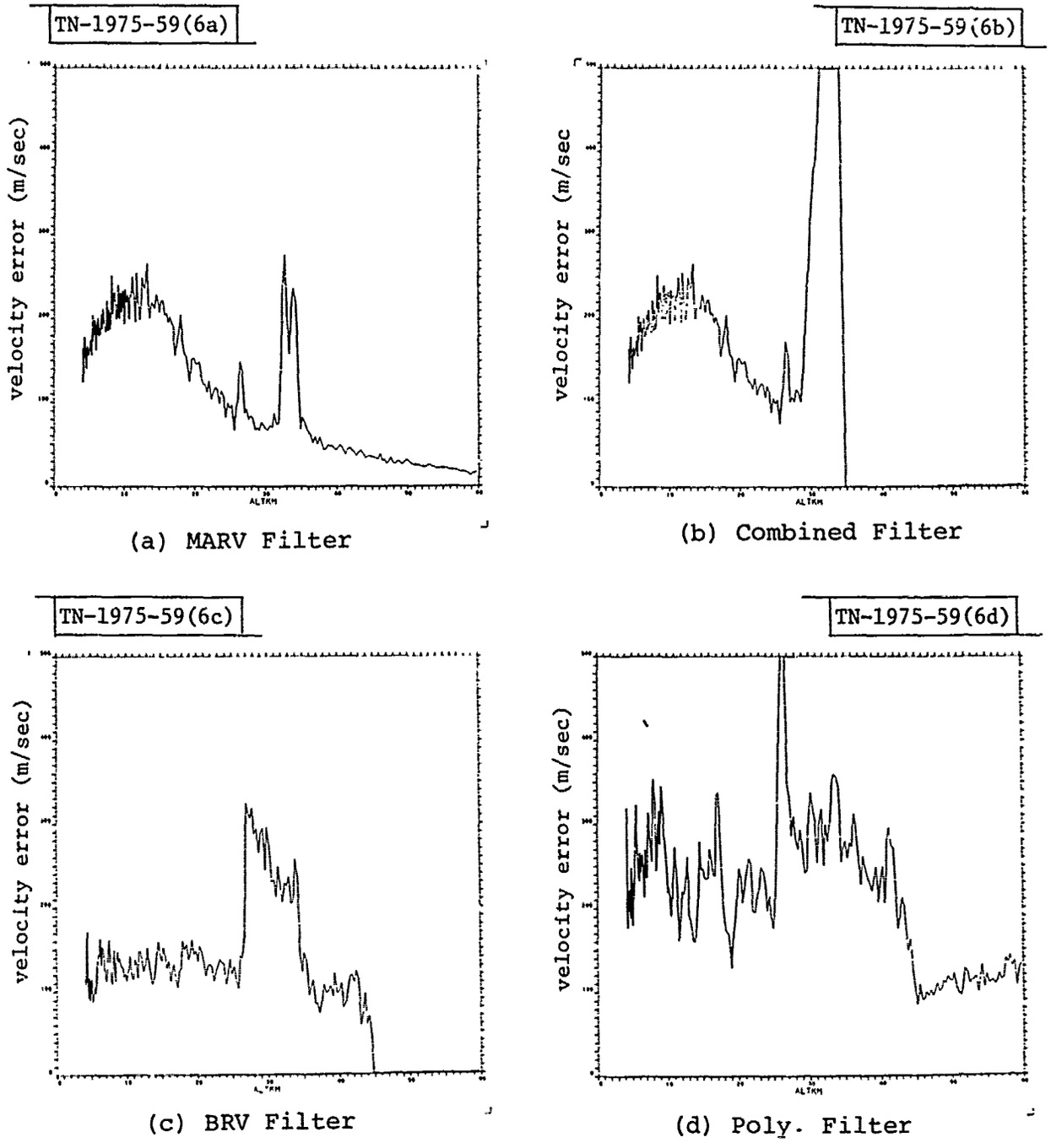

Fig. 6. Velocity estimate rms errors of T2.

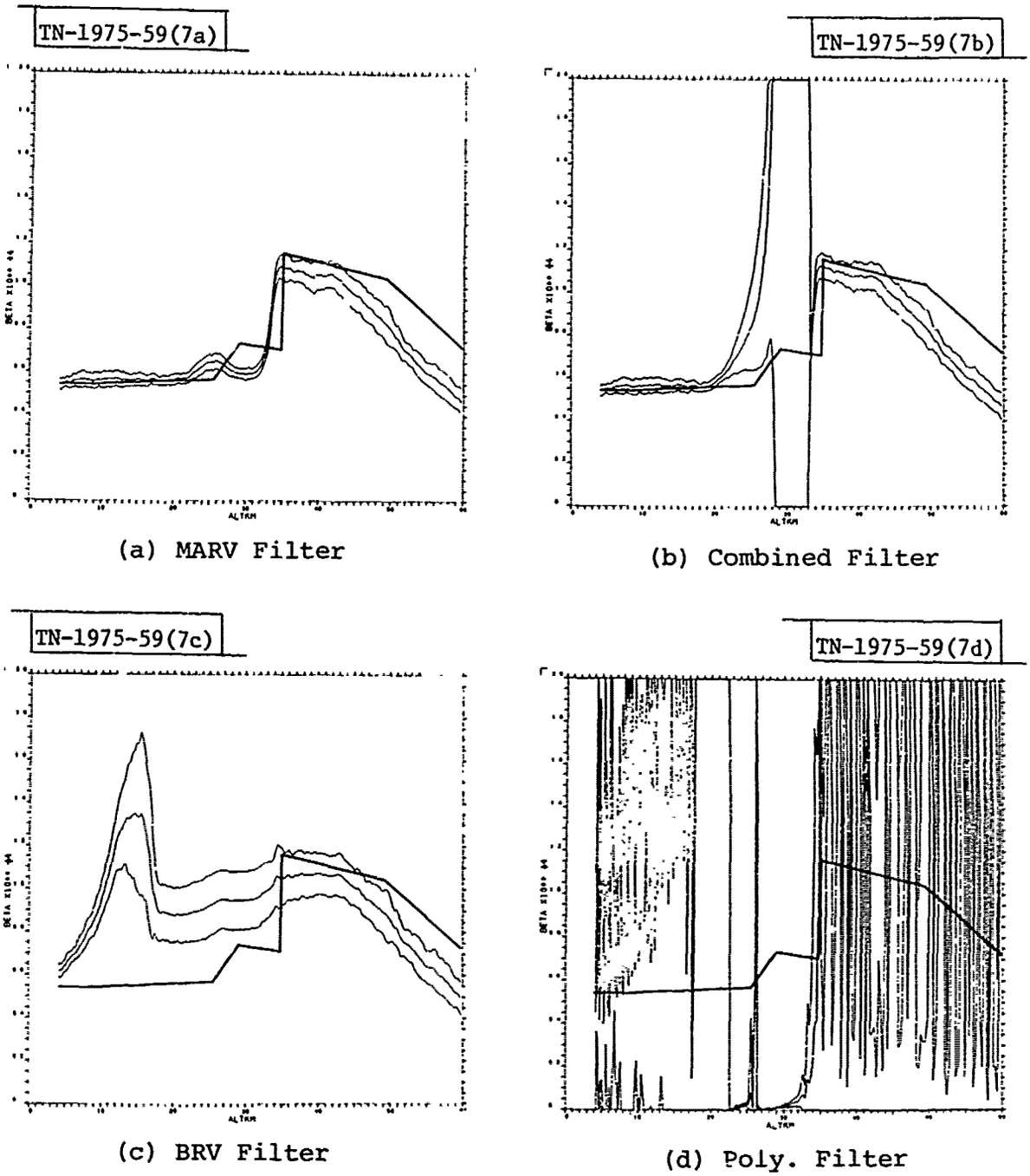

(a) MARV Filter

(b) Combined Filter

(c) BRV Filter

(d) Poly. Filter

Fig. 7. Ballistic coefficient estimate of T2.

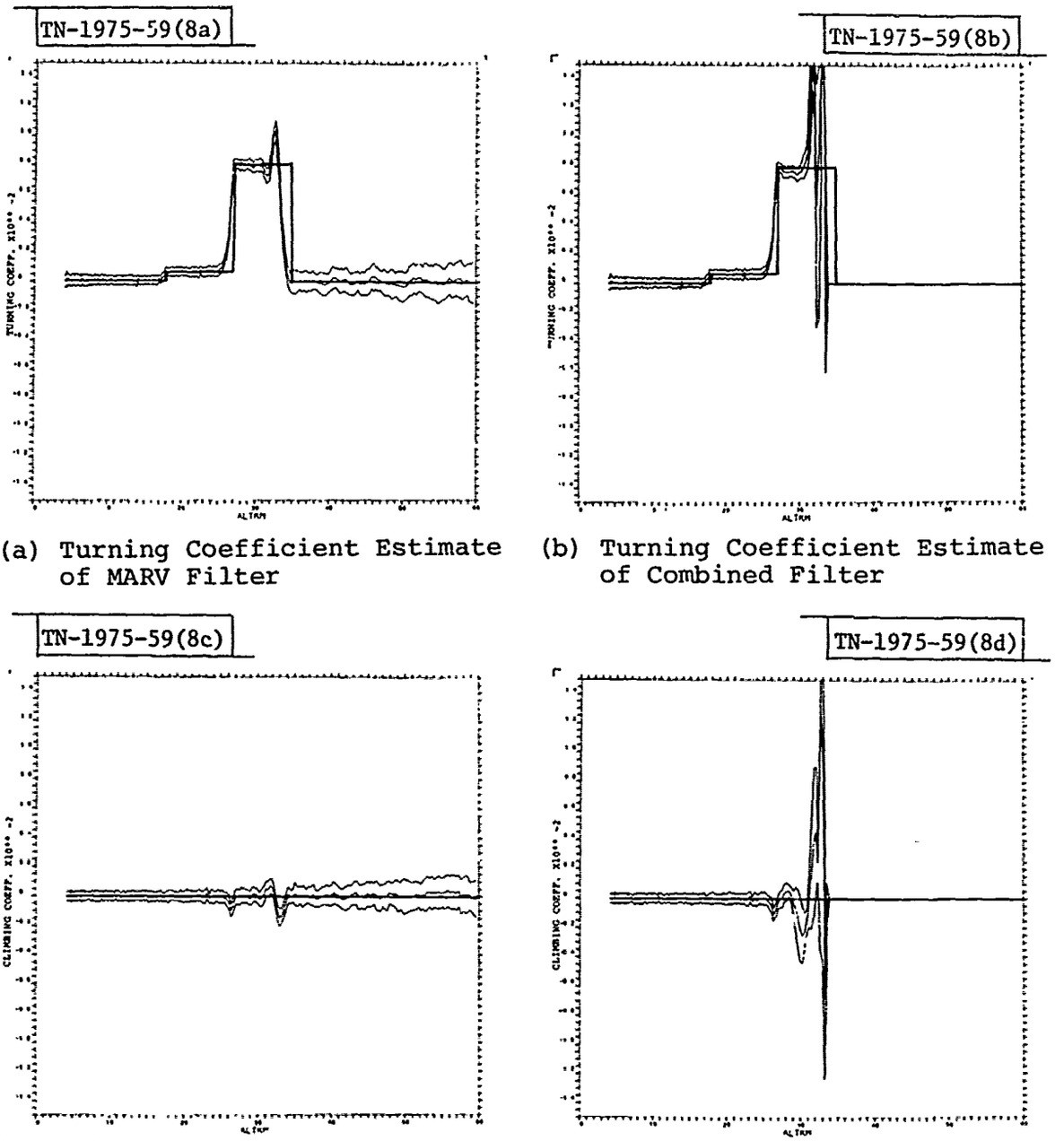

(a) Turning Coefficient Estimate of MARV Filter

(b) Turning Coefficient Estimate of Combined Filter

(c) Climbing Coefficient Estimate of MARV Filter

(d) Climbing Coefficient Estimate of Combined Filter

Fig. 8. Maneuvering parameter estimate of T2.

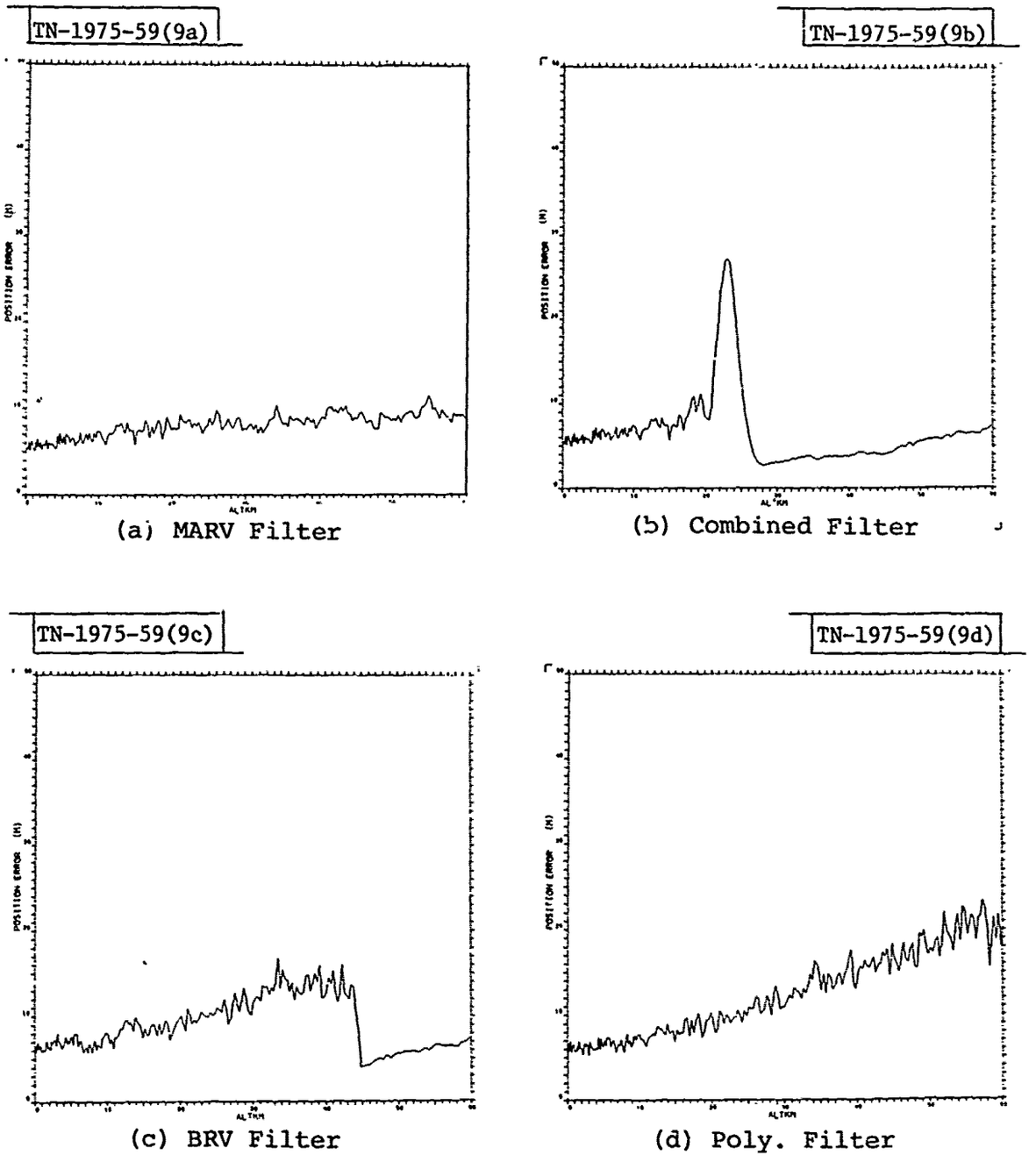

(a) MARV Filter

(b) Combined Filter

(c) BRV Filter

(d) Poly. Filter

Fig. 9. Position estimate rms errors of T3.

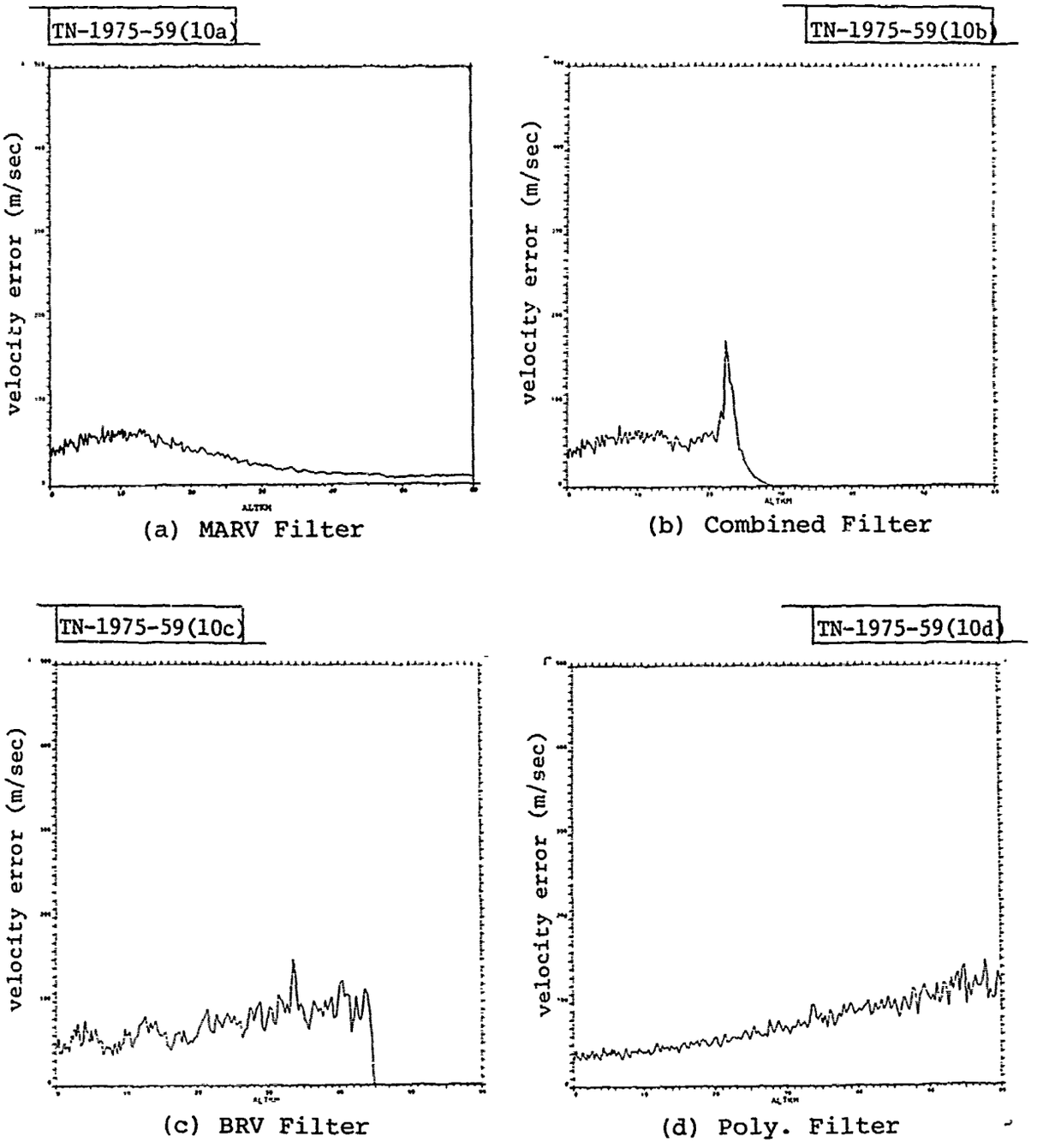

Fig. 10. Velocity estimate rms errors of T3.

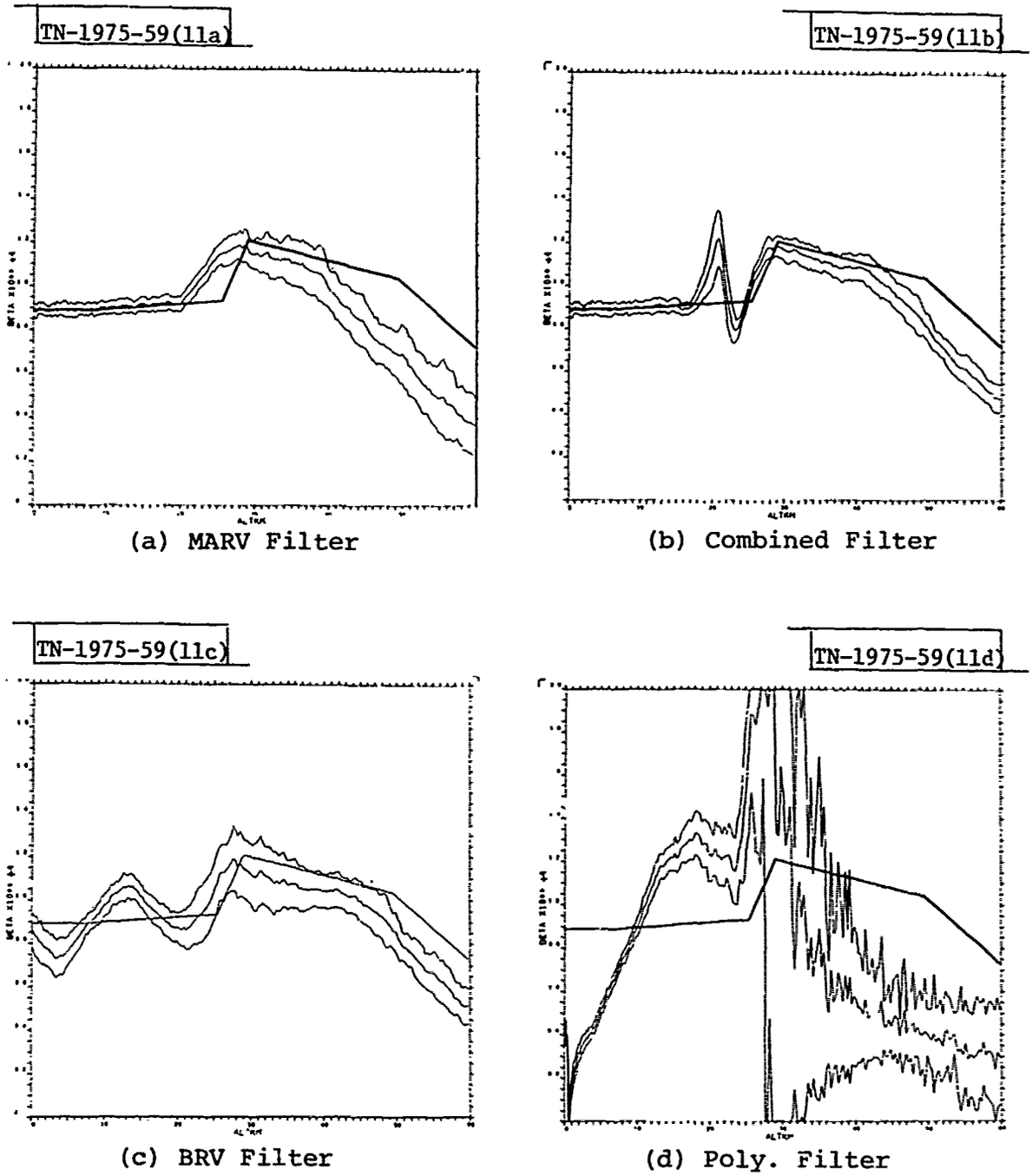

(a) MARV Filter

(b) Combined Filter

(c) BRV Filter

(d) Poly. Filter

Fig. 11. Ballistic coefficient estimate of T3.

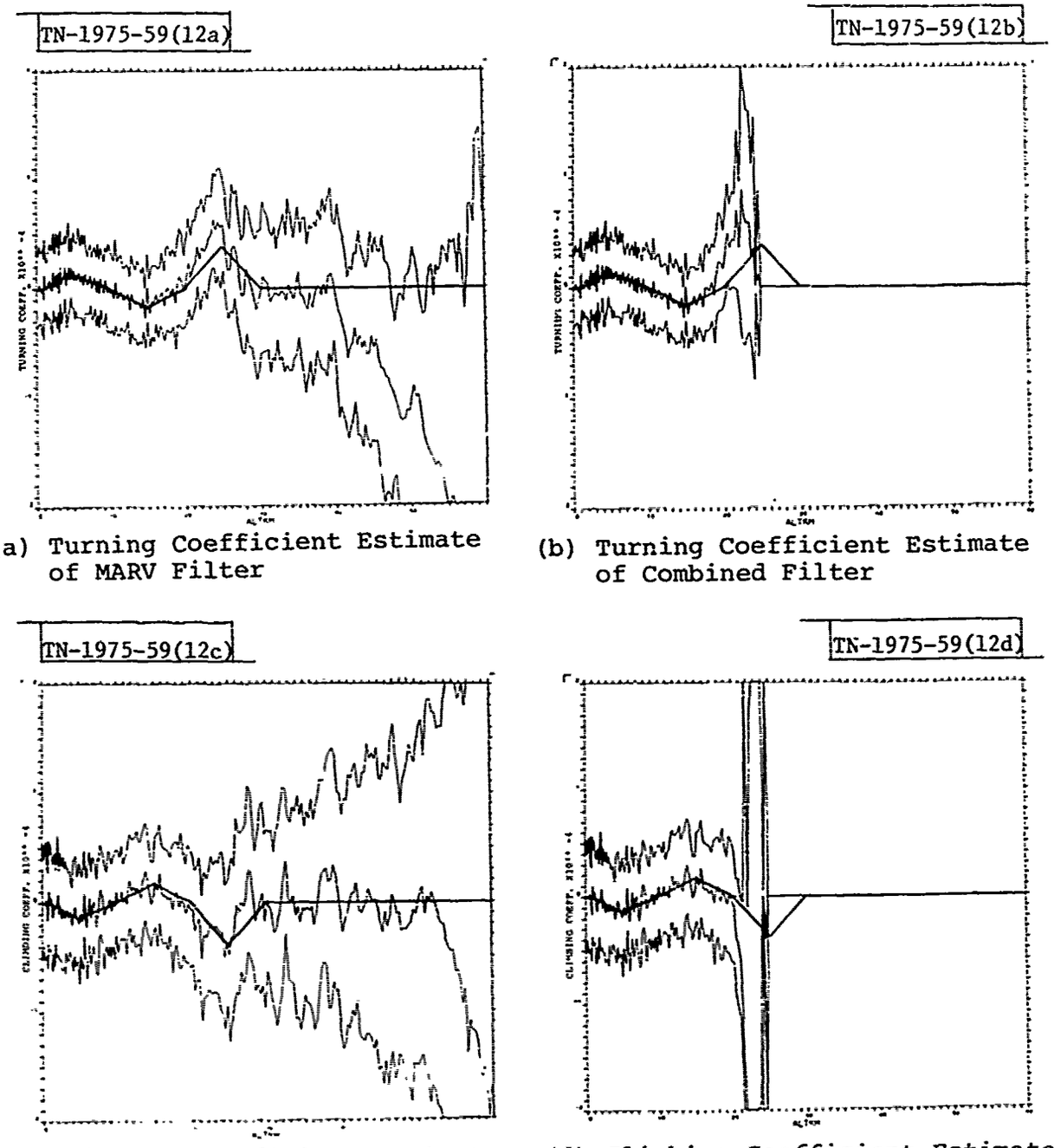

(a) Turning Coefficient Estimate of MARV Filter

(b) Turning Coefficient Estimate of Combined Filter

c) Climbing Coefficient Estimate of MARV Filter

(d) Climbing Coefficient Estimate of Combined Filter

Fig. 12. Maneuvering parameter estimate of T3.

TN-1975-59(13a)

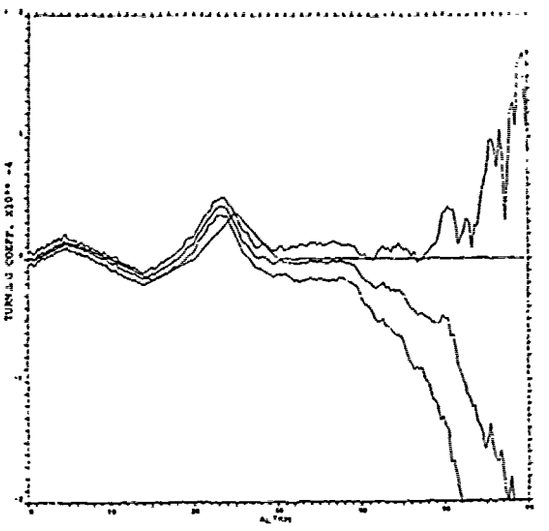

(a) Turning Coefficient

TN-1975-59(13b)

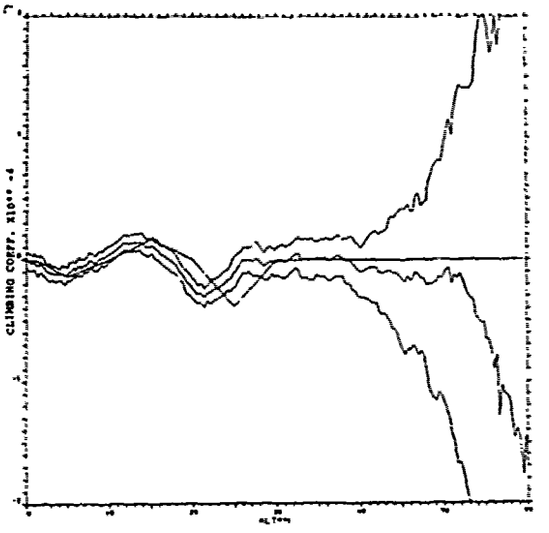

(b) Climbing Coefficient

Fig. 13. Maneuvering parameter estimate of T3 by MARV filter with small process noise.

REFERENCES

1. R. E. Kalman, "A New Approach to Linear Filtering and Prediction Problem," Trans. ASME, J. Basic Engr., Ser. D 82, 34-35 (1960).

2. A. H. Jazwinski, Stochastic Processes and Filtering Theory, (Academic Press, New York, 1970).

3. A. Gelb, Ed., Applied Optimal Estimations (M.I.T. Press, Cambridge, Massachusetts, 1974).

4. M. Gruber, "An Approach to Target Tracking," Technical Note 1967-8, Lincoln Laboratory, M.I.T. (10 February 1971), DDC-AD-654272.

5. R. E. Larson, R. M. Dressler, and R. S. Ratner, "Application of the Extended Kalman Filter to Ballistic Trajectory Estimation," Stanford Research Insititue, Menlo Park, California Final Report (January 1967).

6. R. P. Wishner, R. E. Larson, and M. Athans, "Status of Radar Tracking Algorithm," Proceedings of the Symposium on Nonlinear Estimation Theory and Its Appliation, San Diego, September

10.

11. R. K. Mehra, "A Comparison of Several Nonlinear Filters for Re-entry Vehicle Tracking," IEEE Trans. Automatic Control AC-16, 307-319 (1971).

12. R. A. Singer, "Estimating Optimal Tracking Filter Performance for Manned Maneuvering Targets," IEEE Trans. Aerospace Electron. Systems AES-6, 473-483 (1970).

13. R. A. Singer and K. W. Behnke, "Real-Time Tracking Filter Evaluation and Selection for Tactical Application," IEEE Trans. Aerospace Electron. Systems AES-6, 100-110 (1971).

14. A. H. Jazwinski, "Adaptive Filtering," Automatica, 5, 475-485 (1969).

15. H. L. Van Trees, Detection, Estimation, and Modulation Theory, Vol. I, (Wiley, New York, 1968).

16. R. K. Mehra, "On the Identification of Variances and Adaptive Kalman Filtering," IEEE Trans. Automatic Control AC-15, 175-184 (1970).

17. R. K. Mehra, "Approaches to Adaptive Filtering," IEEE Trans. Automatic Control AC-17, 693-698 (1972).

18. B. Carew and P. R. Belanger, "Identification of Optimum Filter Steady-State Gain for Systems with Unknown Noise Covariances," IEEE Trans Automatic Control AC-18, 582-589 (1973).

19. D. L. Alspach and A. Abiri, "Optimal Nonlinear Estimation for a Linear System with Unknown Plant and Measurement Noise Covariances," Proceedings of Symposium on Nonlinear Estimation Theory, San Diego, September 1972.

20. Y. Bar-Shalom, E. Tse, R. Dressler, "Adaptive Estimation in the Presence of Non-stationary Noises with Unknown Statistics--Application to Maneuvering Targets," Proceedings of Symposium on Nonlinear Estimation Theory, San Diego, September 1973.

21. M. Athans, "The Role of the Stochastic Linear-Quadratic-Gaussian Problem in Control System Design," IEEE Trans. Automatic Control AC-16, 529-552 (1971).

APPENDIX A

Derivation of MARV Differential Equations of Motion

In this Appendix, the MARV equations of motion are derived. A flat, nonrotating earth with constant gravity model is assumed. For the altitude region below 100 km which is our concern, this assumption introduces only small modeling errors while greatly simplifying the equations. It is well known that a ballistic trajectory may be described by the following vector equation

$$\vec{a}(t) = \frac{1}{2}\rho v^2(t)\frac{1}{\beta}\vec{u}_d + \vec{g} \qquad \text{(A.1)}$$

where

$\vec{a}(t)$ is the total acceleration applied on the vehicle

ρ is the air density

$v(t)$ is the magnitude of the vehicle velocity

$\vec{u}_d$ is the unit vector along the drag force direction which is opposite to the velocity vector

$\vec{g}$ is the gravity force vector

β is the zero lift ballistic coefficient defined as $\beta = \frac{m}{C_{d0}A}$ where m=BRV mass, C_{d0}=zero lift drag coefficient, and A=reference area for drag evaluation.

In tracking algorithms, the filter usually estimates the ballistic parameter α which is defined as inverse of β.

When the vehicle undertakes a maneuver, a third force term, lift, is introducted. The lift force is in a plane perpendicular to the velocity vector (Fig. A.1). Before starting the

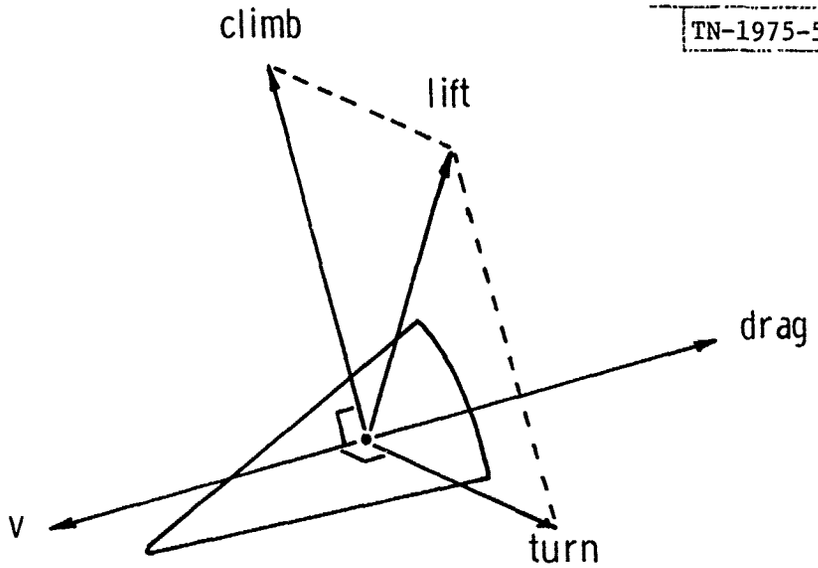

a) lift force is perpendicular to drag force

b) turn and climb forces are components of lift force

c) turn force is on the local horizontal plane

d) turn, climb, and drag forces form an orthogonal coordinate

Fig. A.1. Geometry of lift and drag forces.

MARV equations, it is useful to summarize the concepts associated with lifting bodies. Consider the motion of a point mass in the atmosphere with a velocity v(t). The total drag force is D(t)

$$D(t) = \frac{1}{2}C_d A\rho v^2(t) \qquad (A.2)$$

where C_d = total drag coefficient. Let L(t) denote the lift force. The magnitude of the lift force is

$$L(t) = \frac{1}{2} C_L A\rho v^2(t) \qquad (A.3)$$

where C_L = lift coefficient. The lift vector, L(t), is always perpendicular to the drag force D(t), as shown in Fig. A.1.

A lifting body contributes extra drag. It is common practice to present this relationship between total drag D(t) and total lift, L(t), by means of the so-called parabolic polar, which is expressed by the equation

$$C_d = C_{d0} + kC_L^2$$

where

C_{d0} = zero lift drag coefficient (i.e., the one that characterizes a BRV)

k = constant that depends on the body

The production of different lift forces is accomplished by changing the lift coefficient C_L of the body. However, there is a specific value for the lift coefficient denoted by C_L^* that maximizes the so-called lift-to-drag ratio.

$$\text{Lift-to-drag ratio} \triangleq \frac{L(t)}{D(T)} = \frac{C_L}{C_D}$$

$$= \frac{C_L}{C_{d0}+kC_L^2}$$

It is easily found that this value C_L^* of the lift coefficient is

$$C_L^* = \frac{C_{d0}}{k}$$

which leads to

$$\text{maximum lift-to-drag ratio} = \frac{1}{2\sqrt{kC_{d0}}}$$

Another common practice is to express C_L in terms of C_L^* by the so-called lift-parameter λ

$$C_L(t) \triangleq \lambda(t) C_L^*; \quad 0 \leq \lambda(t) \leq 1$$

Using these notations we can write:

$$\text{Total Drag Force} = D(t) = \frac{1}{2}\rho A C_{d0}\left(1+\lambda^2(t)\right) v^2(t) \qquad (A.4)$$

$$\text{Total Lift Force} = L(t) = \frac{1}{2}\rho A C_L^* \lambda(t) v^2(t) \qquad (A.5)$$

Note that:

$$\text{Zero Lift Drag Force} = \frac{1}{2}\rho A C_{d0} v^2(t)$$

$$\text{Lift-Induced Drag Force} = \frac{1}{2}\rho A C_{d0} \lambda^2(t) v^2(t)$$

Using the above discussions, the maneuvering trajectory may be described by the follcwing vector equation

$$\vec{a}(t) = \frac{1}{2}\rho v^2(t)\left(\alpha(1+\lambda^2)\vec{u}_d + \lambda\delta_\ell \vec{u}_\ell\right) + \vec{g} \qquad (A.6)$$

where $\alpha = \frac{1}{\beta} = \frac{C_{d0}A}{m}$

$$\delta_\ell = \frac{C_L^* A}{m}$$

Notice that this equation is written free of coordinate systems. Once a coordinate system is chosen, set of state differential equations may be written for simulation and filter realization. The lift vector is on the plane perpendicular to the drag vector. In order to locate the lift vector on the plane, a reference quantity is necessary. If a Cartesian coordinate is used and the lift vector reference is chosen to be the angle between the lift vector and the local horizontal plane, Eq. (2.1) results. As discussed in the text, one can also decompose the lift vector into a turn force and a climb force. Using this decomposition, Eq. (A.6) may be rewritten as

$$\vec{a}(t) = \frac{1}{2}\rho v^2(t)\left(\alpha(1+\lambda^2)\vec{u}_d + \lambda\delta_t\vec{u}_t + \lambda\delta_c\vec{u}_c\right) + \vec{g} \qquad (A.7)$$

The corresponding state equations of (A.7) in a Cartesian coordinate is Eq. (2.2).

APPENDIX B

Range, Azimuth, Elevation, and Range Rate Estimate Errors of Numerical Examples

In this Appendix, figures showing range, azimuth, elevation, and range rate estimation errors of numerical examples given in this report are presented. Results of using trajectories T1, T2, and T3 are shown in Figs. B.1 to B.4, B.5 to B.8, and B.9 to B.12, respectively. Errors shown in each figure include estimate bias and one standard deviation interval developed through 40 Monte Carlo runs of the algorithm. Bias error is defined as the estimated value minus the true value.

These results are included for reference purposes. Many filter responses to the target maneuvering may be understood by examining these results. For example, Fig. B.4(b) presents the range rate estimate error of T2 made by the adaptive BRV filter. Notice that a large negative bias appears when the RV undergoes maneuvering. When the RV turns sharply away from the radar, the magnitude of the true range rate is rapidly decreasing. The BRV filter which does not have the lift force component modeled estimates the range rate corresponding to a vector sum of the drag and lift forces. This range rate bias then in turn causes the β estimate to be biased as shown in Fig. 7(c). The MARV filter which has the lift force modeled has an unbiased range rate estimate. The estimation variance is high due to the process noise introduced in the drag/lift parameter states.

Other filter responses may be examined by using similar observations.

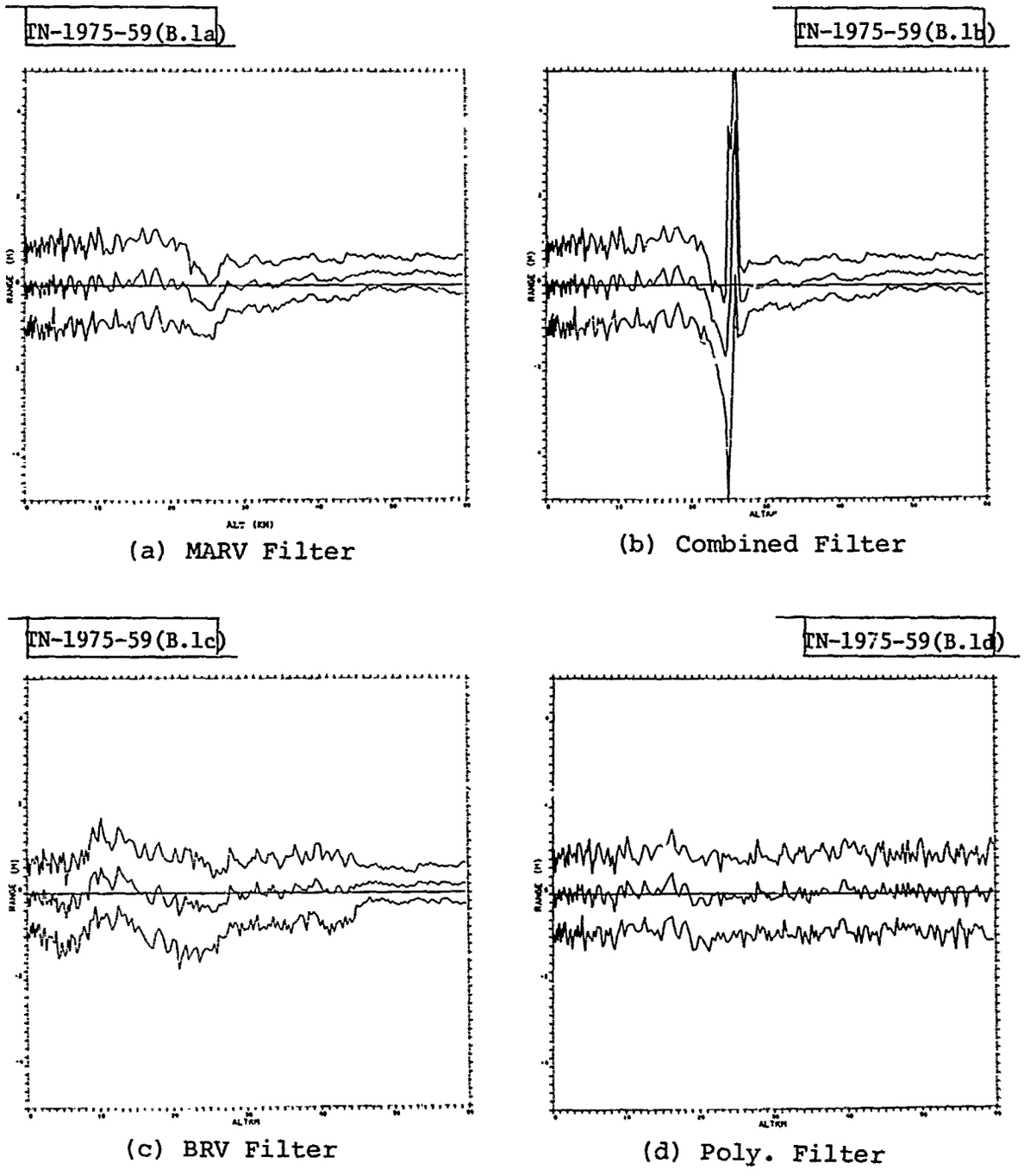

(a) MARV Filter

(b) Combined Filter

(c) BRV Filter

(d) Poly. Filter

Fig. B.1. Range estimate errors of T1.

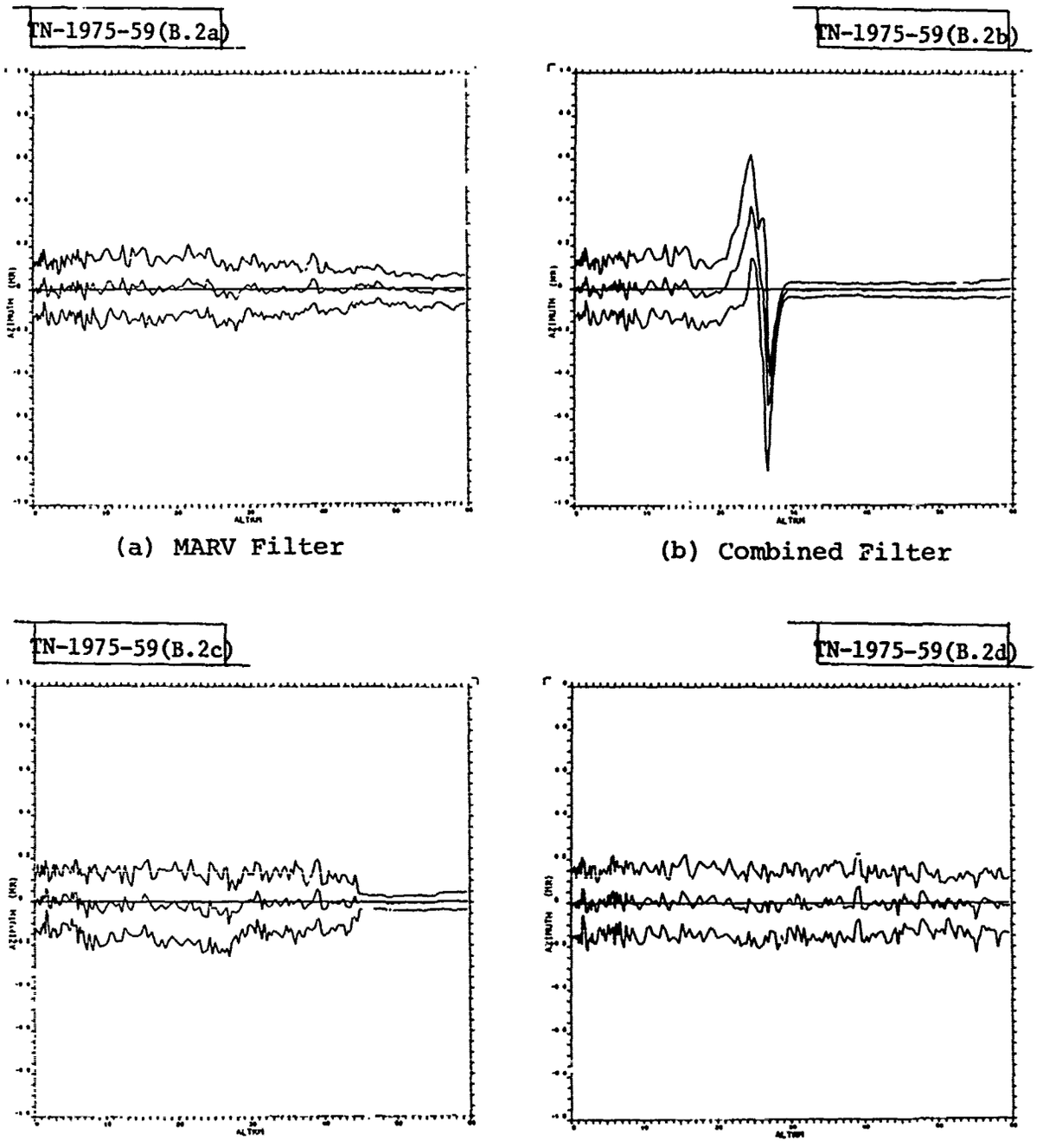

(a) MARV Filter

(b) Combined Filter

(c) BRV Filter

(d) Poly. Filter

Fig. B.2. Azimuth estimate errors of T1.

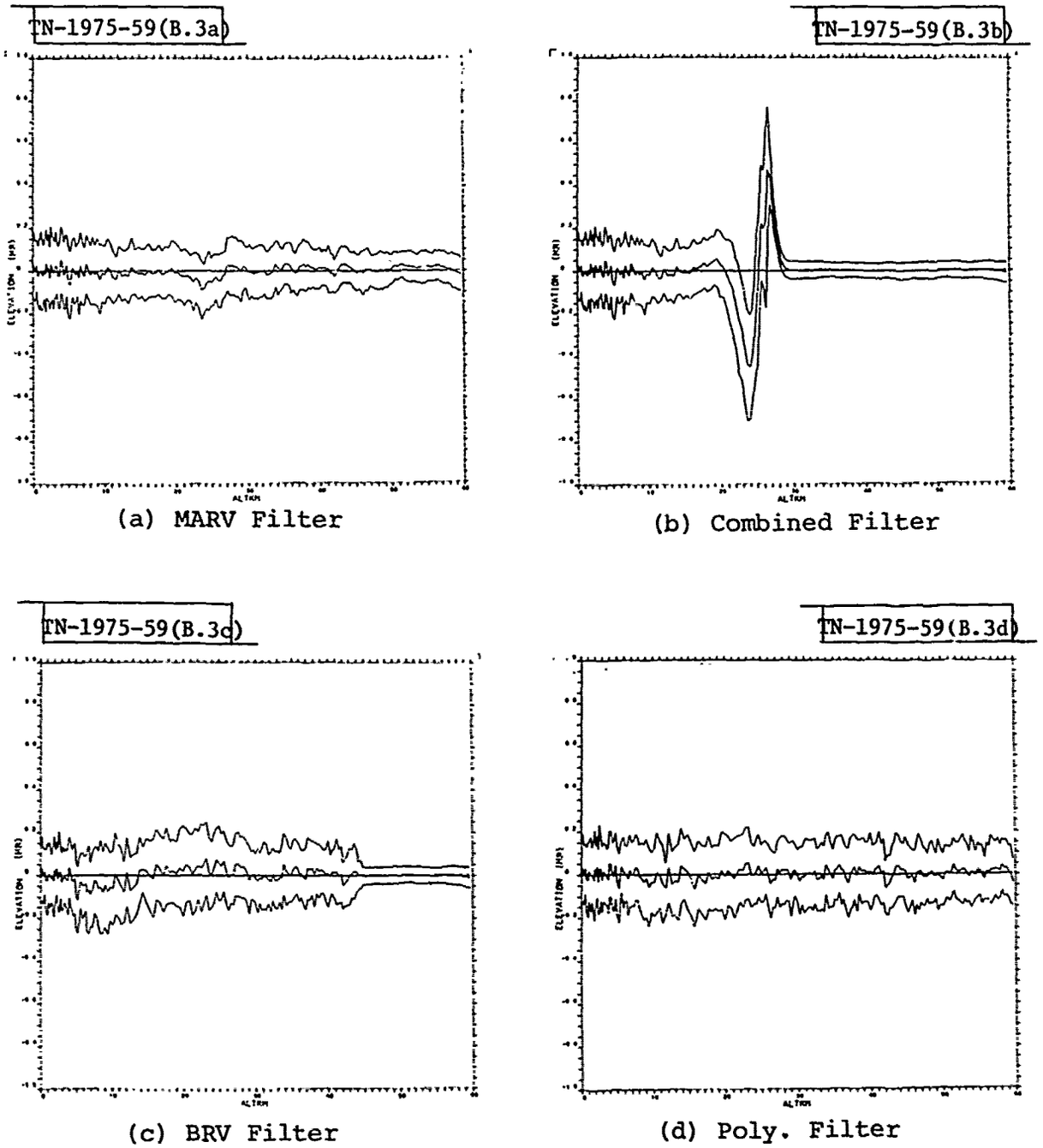

(a) MARV Filter

(b) Combined Filter

(c) BRV Filter

(d) Poly. Filter

Fig. B.3. Elevation estimate errors of T1.

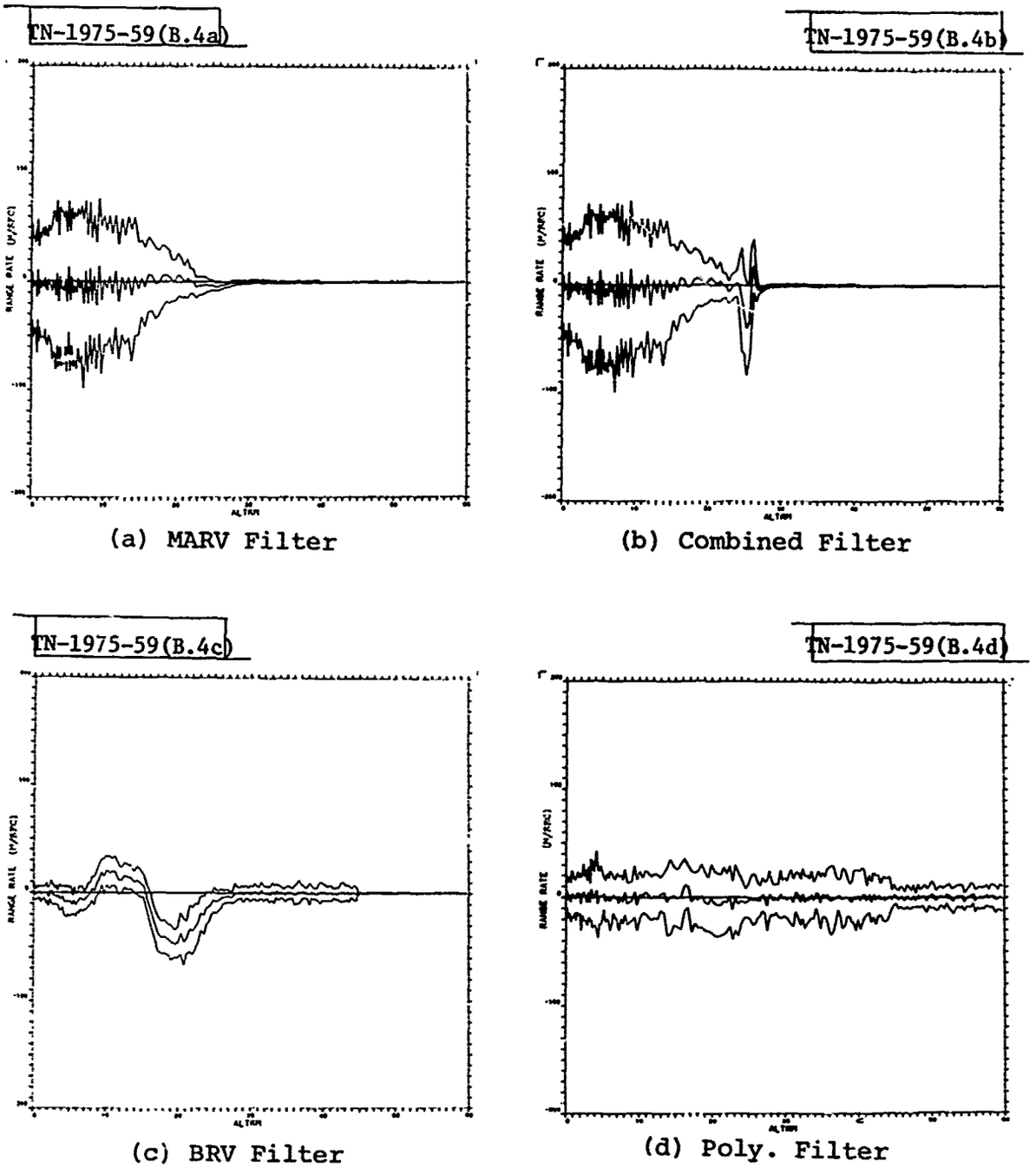

(a) MARV Filter

(b) Combined Filter

(c) BRV Filter

(d) Poly. Filter

Fig. B.4. Range rate estimate errors of T1.

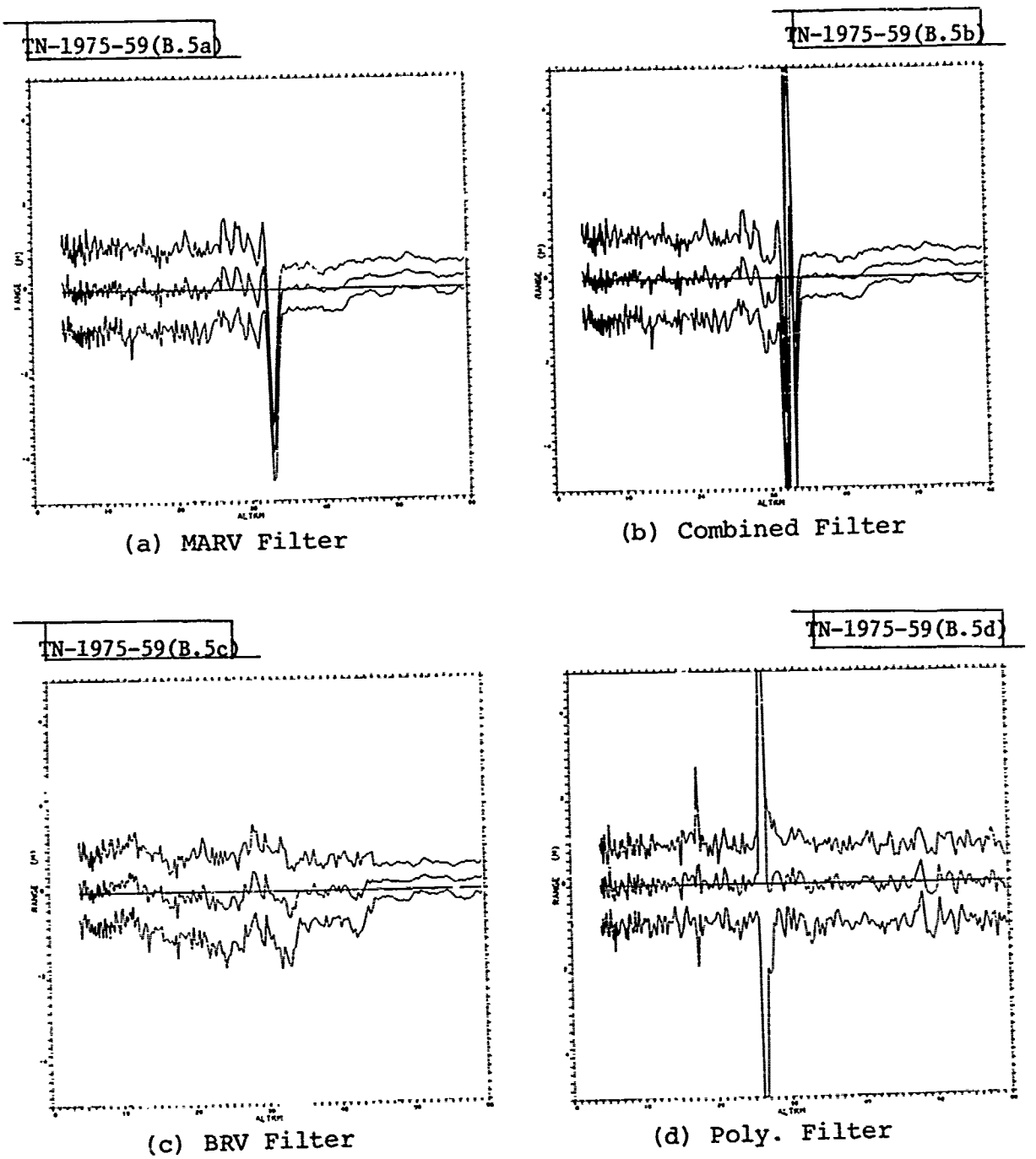

(a) MARV Filter

(b) Combined Filter

(c) BRV Filter

(d) Poly. Filter

Fig. B.5. Range estimate errors of T2.

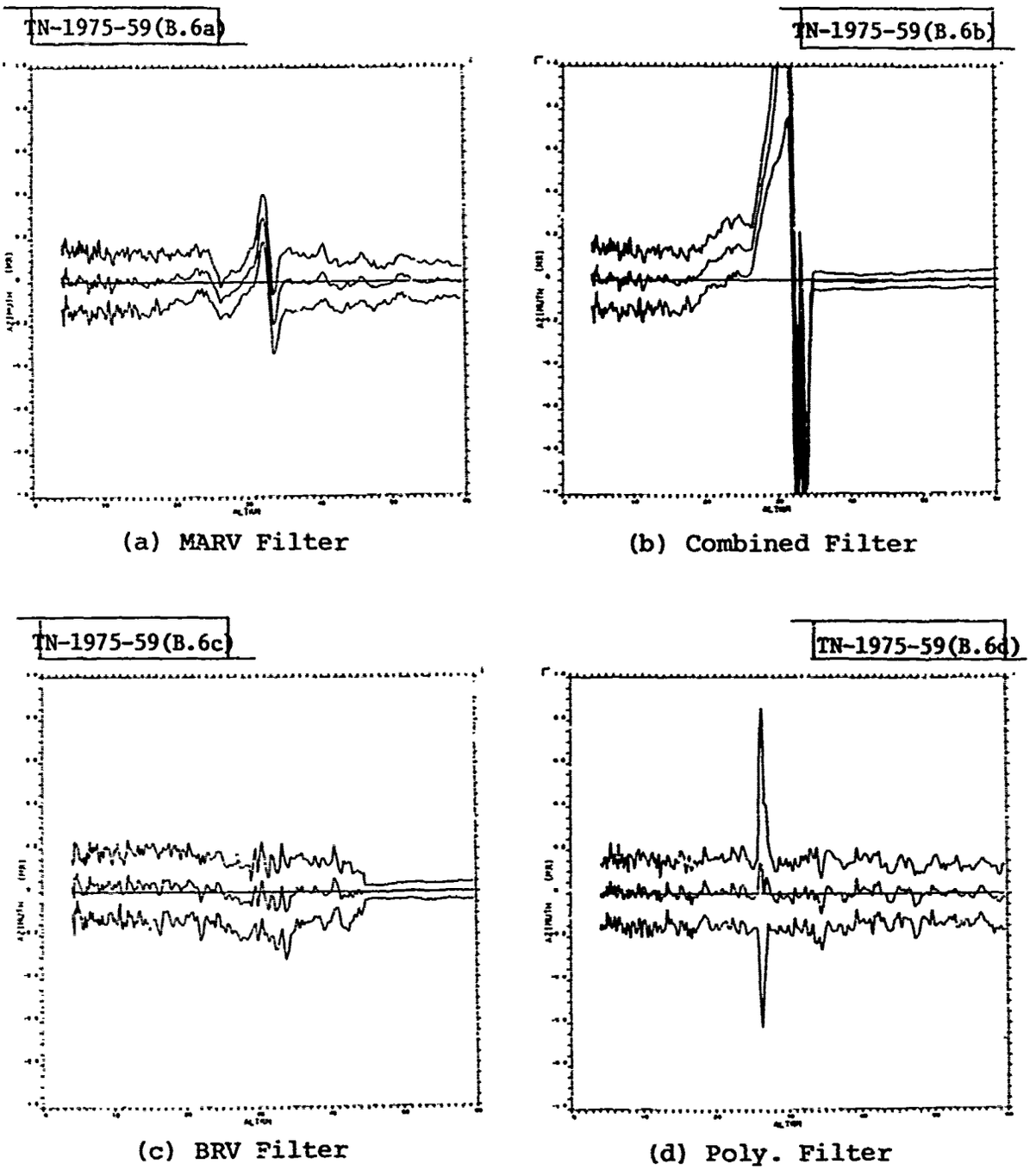

(a) MARV Filter

(b) Combined Filter

(c) BRV Filter

(d) Poly. Filter

Fig. B.6. Azimuth estimate errors of T2.

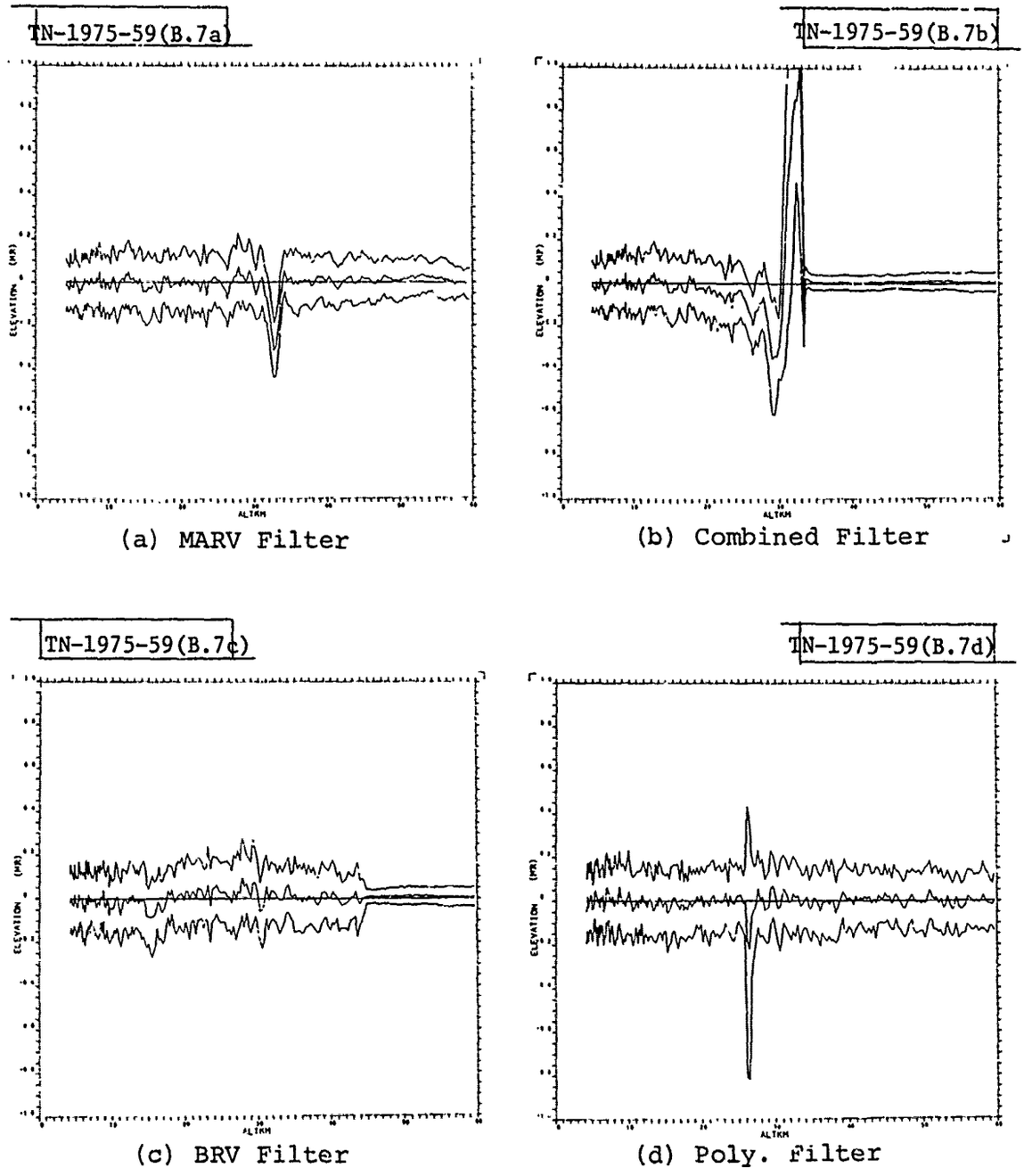

(a) MARV Filter (b) Combined Filter

(c) BRV Filter (d) Poly. Filter

Fig. B.7. Elevation estimate errors of T2.

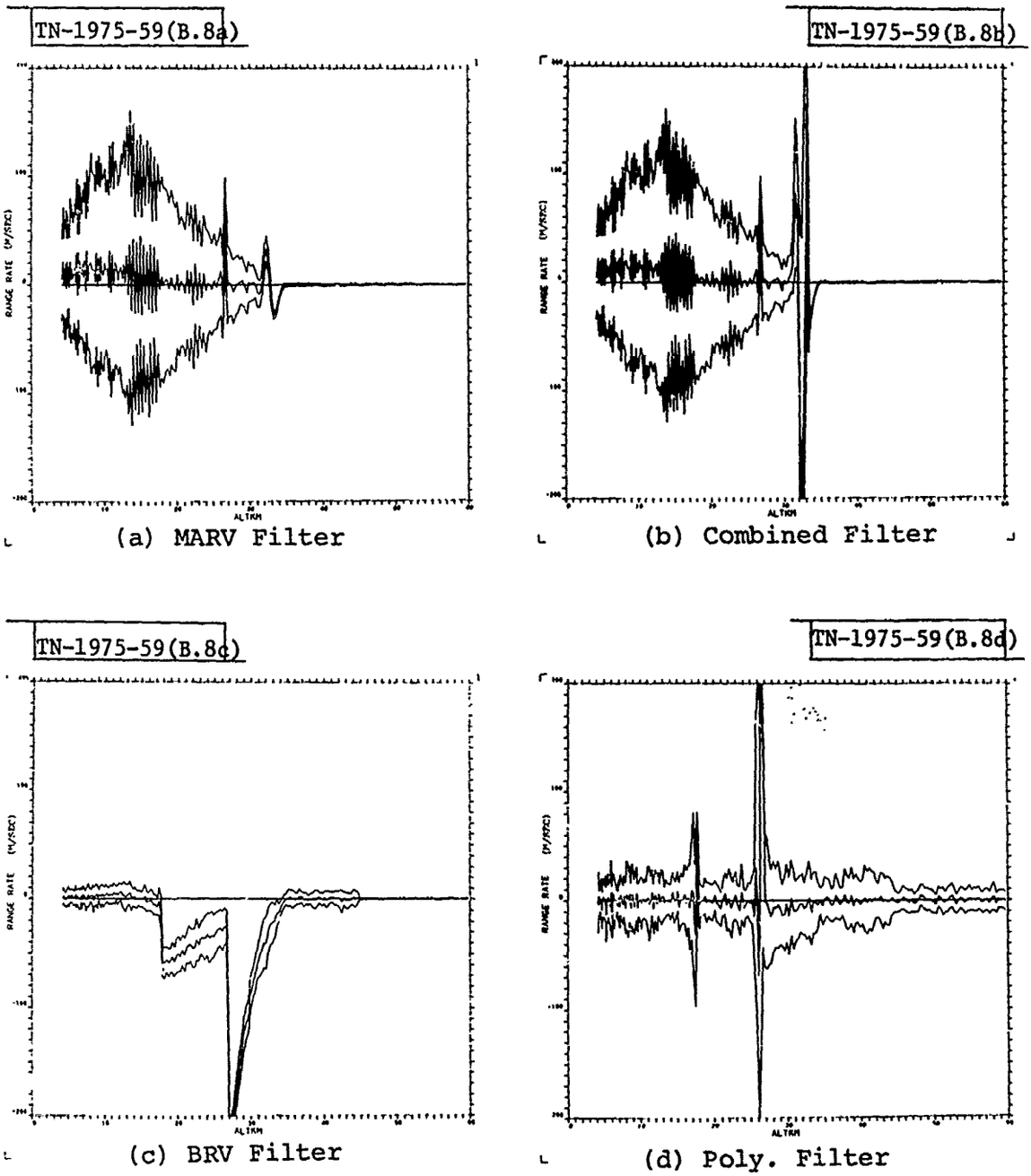

(a) MARV Filter

(b) Combined Filter

(c) BRV Filter

(d) Poly. Filter

Fig. B.8. Range rate estimate errors of T2.

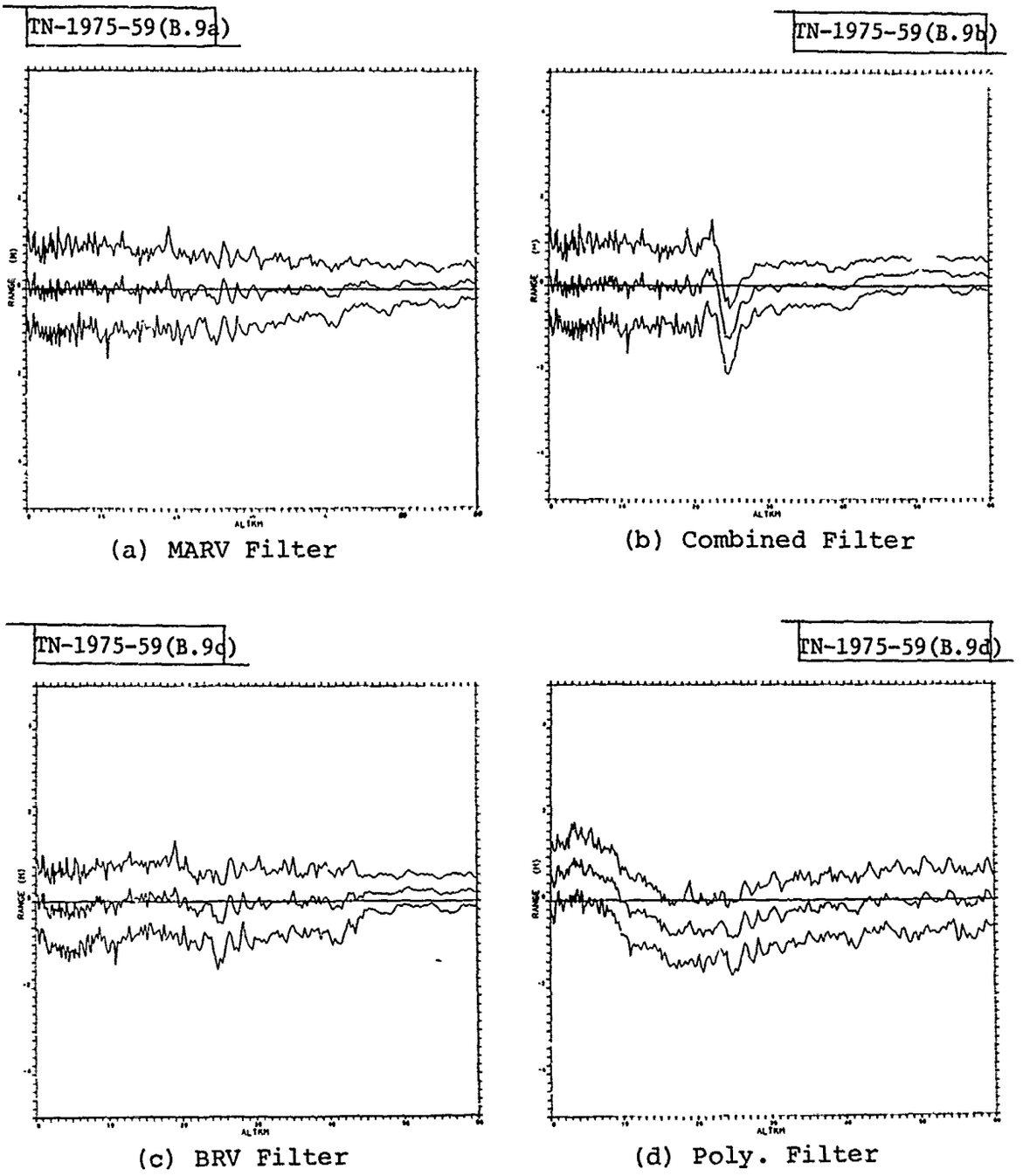

(a) MARV Filter

(b) Combined Filter

(c) BRV Filter

(d) Poly. Filter

Fig. B.9. Range estimate errors of T3.

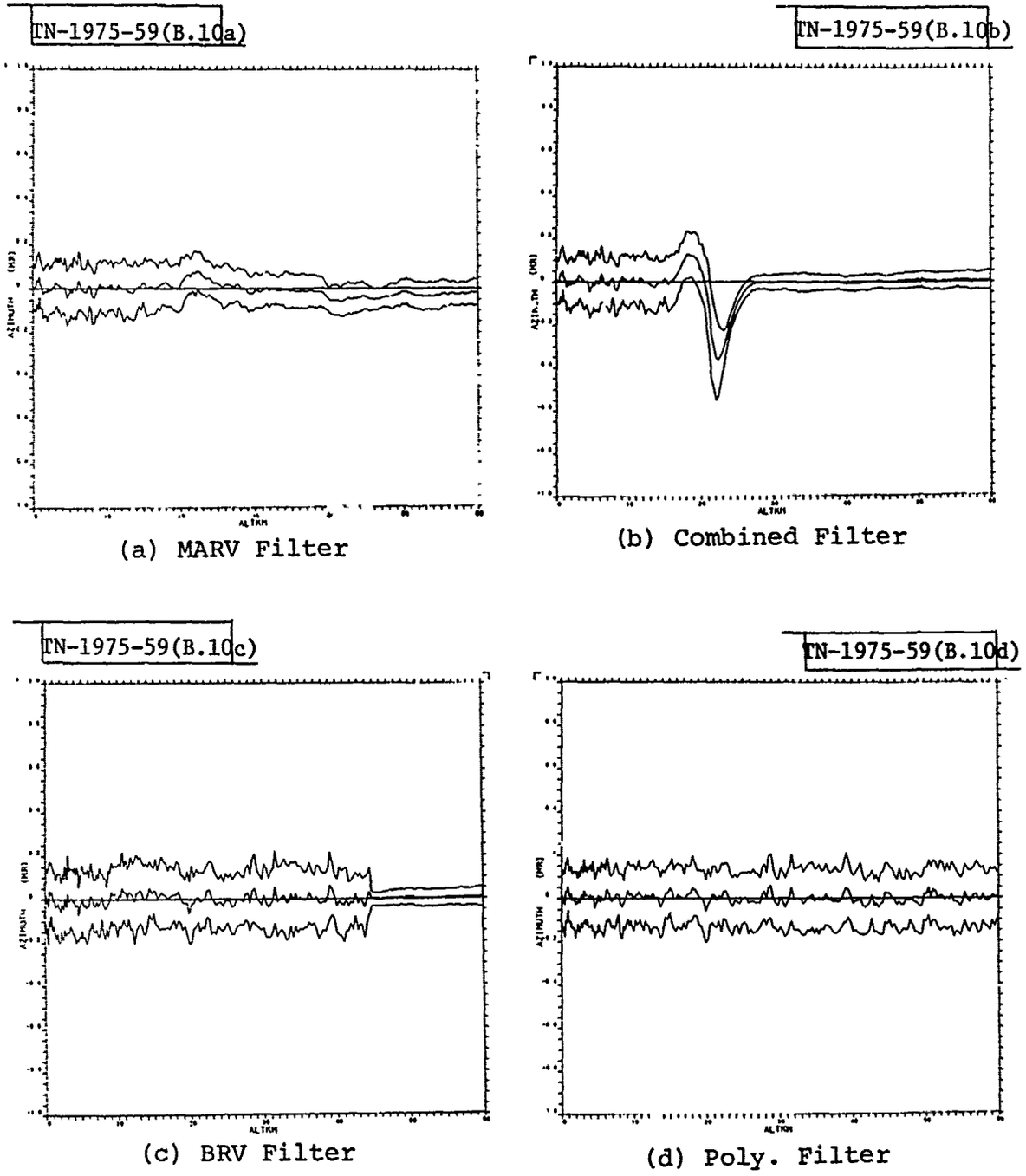

(a) MARV Filter

(b) Combined Filter

(c) BRV Filter

(d) Poly. Filter

Fig. B.10. Azimuth estimate errors of T3.

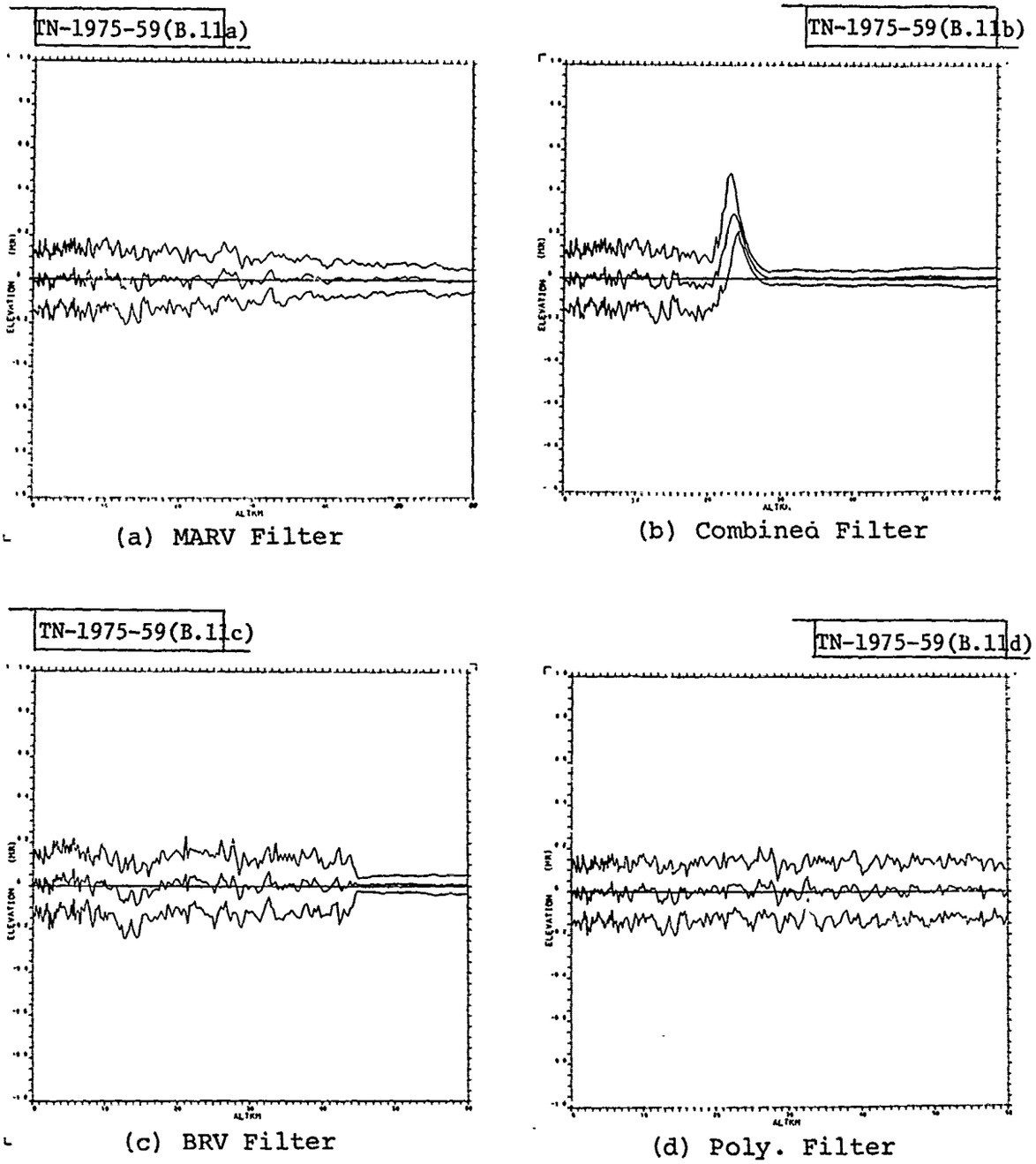

(a) MARV Filter (b) Combined Filter

(c) BRV Filter (d) Poly. Filter

Fig. B.11. Elevation estimate errors of T3.

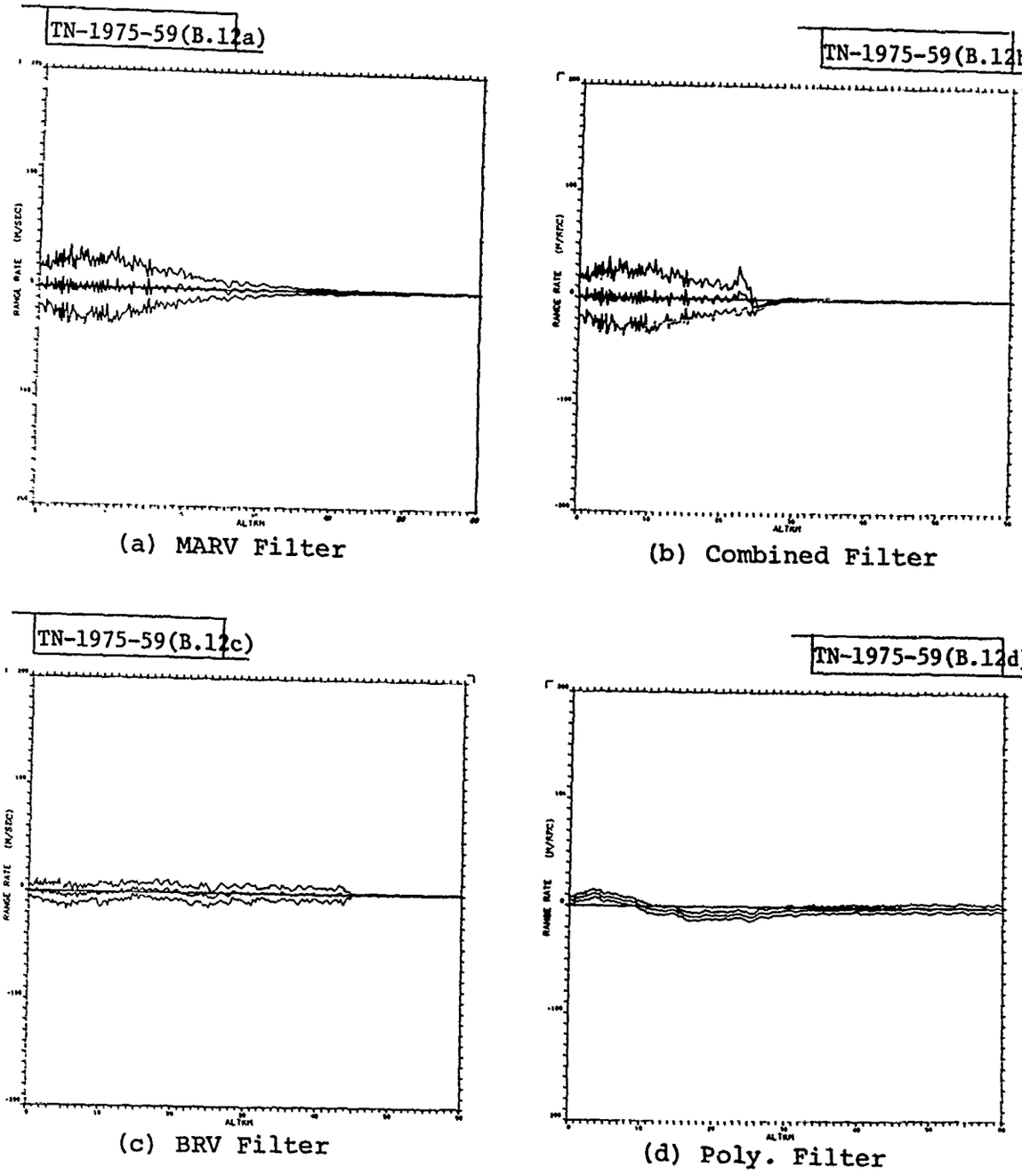

(a) MARV Filter

(b) Combined Filter

(c) BRV Filter

(d) Poly. Filter

Fig. B.12. Range rate estimate errors of T3.

UNCLASSIFIED

SECURITY CLASSIFICATION OF THIS PAGE *(When Data Entered)*

(19) REPORT DOCUMENTATION PAGE	READ INSTRUCTIONS BEFORE COMPLETING FORM
1. REPORT NUMBER (18) ESD-TR-75-320 — 2. GOVT ACCESSION NO. (14) TN-1975-59	3. RECIPIENT'S CATALOG NUMBER
4. TITLE (and Subtitle) (6) Application of Adpative Filtering Methods to Maneuvering Trajectory Estimation	5. TYPE OF REPORT & PERIOD COVERED (9) Technical Note
	6. PERFORMING ORG. REPORT NUMBER Technical Note 1975-59
7. AUTHOR(s) Chang, Chaw-Bing, Whiting, Robert H., and Athans, Michael	8. CONTRACT OR GRANT NUMBER(s) (15) F19628-76-C-0002
9. PERFORMING ORGANIZATION NAME AND ADDRESS Lincoln Laboratory, M.I.T. P.O. Box 73 Lexington, MA 02173	10. PROGRAM ELEMENT, PROJECT, TASK AREA & WORK UNIT NUMBERS Project No. 8X363304D215
11. CONTROLLING OFFICE NAME AND ADDRESS Ballistic Missile Defense Program Office Department of the Army 1320 Wilson Boulevard Arlington, VA 22209	12. REPORT DATE (11) 24 November 1975 — (12) 74p. 13. NUMBER OF PAGES 76
14. MONITORING AGENCY NAME & ADDRESS *(if different from Controlling Office)* Electronic Systems Division Hanscom AFB Bedford, MA 01731	15. SECURITY CLASS. *(of this report)* Unclassified 15a. DECLASSIFICATION DOWNGRADING SCHEDULE

16. DISTRIBUTION STATEMENT *(of this Report)*

Distribution limited to U.S. Government agencies only; test and evaluation; 28 November 1975. Other requests for this document must be referred to ESD/TML (Lincoln Laboratory), Hanscom AFB, MA 01731.

17. DISTRIBUTION STATEMENT *(of the abstract entered in Block 20, if different from Report)*

(10) Chaw-Bing Chang, Robert H. Whiting, Michael Athans

18. SUPPLEMENTARY NOTES

None (16) DH-8-X-363304-D-215

19. KEY WORDS *(Continue on reverse side if necessary and identify by block number)*

re-entry vehicle tracking
radar measurements
Kalman filters
adaptive filtering
trajectory estimation
MARV
maneuver detection

20. ABSTRACT *(Continue on reverse side if necessary and identify by block number)*

The purpose of this report is to examine several modifications of extended Kalman filters which can be used to estimate the position, velocity, and other key parameters associated with maneuvering re-entry vehicles. These filters will be described and discussed in terms of the fundamental problems of modeling accuracy, filter sophistication, and the real-time computational requirements. A nine-state, extended Kalman filter based upon the maneuvering vehicle dynamics is compared with several other candidate filters. These candidate filters include a simple filter based upon polynomial dynamics decoupled with respect to the coordinates and a more complex, fully coupled, seven-state, extended Kalman filter based upon a ballistic re-entry vehicle dynamics. Techniques which adaptively increase the process noise to compensate for modeling errors during the maneuvers are examined.

DD FORM 1 JAN 73 1473 EDITION OF 1 NOV 65 IS OBSOLETE

UNCLASSIFIED

SECURITY CLASSIFICATION OF THIS PAGE *(When Data Entered)*

207650

4/B

SUPPLEMENTARY

INFORMATION

DEPARTMENT OF THE AIR FORCE
HEADQUARTERS ELECTRONIC SYSTEMS DIVISION (AFSC)
HANSCOM AIR FORCE BASE, MASSACHUSETTS 01731

AD-B008137

REPLY TO ATTN OF: TOFL (Lincoln Laboratory) 17 December 1981

SUBJECT: Change in Distribution Statement, AD-B008137L/Deletion of References

TO: DTIC/DDA2
Attn: Mrs. Crumbacker

1. Per our discussion on 16 December, request that the subject report (ESD-TR-75-320, Lincoln Lab TN 1975-59, Application of Adaptive Filtering Methods to Maneuvering Trajectory Estimation, 24 Nov 75) be changed from Distribution Statement B to A.

2. Approval for this change was based on deleting references 7,8,9, and 10 on page 48 of the report (all are S-FRD). Would you please delete those from your file copy.

Raymond L. Loiselle
RAYMOND L. LOISELLE, Lt Colonel, USAF
Chief, Lincoln Laboratory Project Office

Cy to: LL Distr/W. Hill
LL Gp 32/C.B. Chang
AFGL/SULL